

Review

Open Access



# Single-atom catalysts in the photothermal catalysis: fundamentals, mechanisms, and applications in VOCs oxidation

Ying Feng<sup>1,2</sup>, Peiqi Chu<sup>1,2</sup>, Zhiquan Hou<sup>1,2</sup>, Linke Wu<sup>1,2</sup>, Yuxi Liu<sup>1,2</sup>, Jiguang Deng<sup>1,2,3,\*</sup> , Hongxing Dai<sup>1,2,\*</sup>

<sup>1</sup>Beijing Key Laboratory for Green Catalysis and Separation, Key Laboratory of Advanced Functional Materials, Ministry of Education, Department of Chemical Engineering and Technology, College of Materials Science and Engineering, Beijing University of Technology, Beijing 100124, China.

<sup>2</sup>Key Laboratory of Beijing on Regional Air Pollution Control, College of Environmental Science and Engineering, Beijing University of Technology, Beijing 100124, China.

<sup>3</sup>Center of Excellence for Environmental Safety and Biological Effects, College of Chemistry and Life Science, Beijing University of Technology, Beijing 100124, China.

**\*Correspondence to:** Prof. Jiguang Deng, Prof. Hongxing Dai, Beijing Key Laboratory for Green Catalysis and Separation, Key Laboratory of Advanced Functional Materials, Ministry of Education, Department of Chemical Engineering and Technology, College of Materials Science and Engineering, Beijing University of Technology, No.100 Pingleyuan, Chaoyang District, Beijing 100124, China. E-mail: jgdeng@bjut.edu.cn; hxdai@bjut.edu.cn

**How to cite this article:** Feng, Y.; Chu, P.; Hou, Z.; Wu, L.; Liu, Y.; Deng, J.; Dai, H. Single-atom catalysts in the photothermal catalysis: fundamentals, mechanisms, and applications in VOCs oxidation. *Chem. Synth.* 2025, 5, 64. <https://dx.doi.org/10.20517/cs.2024.211>

**Received:** 31 Dec 2024 **First Decision:** 10 Feb 2025 **Revised:** 18 Feb 2025 **Accepted:** 27 Feb 2025 **Published:** 17 Jul 2025

**Academic Editor:** Jin Xie **Copy Editor:** Pei-Yun Wang **Production Editor:** Pei-Yun Wang

## Abstract

Environmental pollution and energy scarcity are the big challenges for the development of contemporary society. The significant rise in global temperature further underscores the importance of adopting sustainable and clean energy sources for environmental purification. This review focuses on the photothermal catalytic oxidation technology, which combines the low energy consumption of photocatalysis with the high efficiency of thermocatalysis, demonstrating substantial potential in the removal of volatile organic compounds (VOCs). It systematically summarizes the research progress in the removal of VOCs by the photothermal catalytic methods over the past five years, and on the basis of the fundamental principles of photothermal catalysis, this review provides an in-depth analysis of the design principles of single-atom catalysts, reaction mechanisms, and their prospects in VOCs purification. The research emphasis includes the mechanisms of photothermic action, strategies for catalyst design, performance outcomes, and the limitations and challenges faced by the single-atom



© The Author(s) 2025. **Open Access** This article is licensed under a Creative Commons Attribution 4.0 International License (<https://creativecommons.org/licenses/by/4.0/>), which permits unrestricted use, sharing, adaptation, distribution and reproduction in any medium or format, for any purpose, even commercially, as long as you give appropriate credit to the original author(s) and the source, provide a link to the Creative Commons license, and indicate if changes were made.



photothermal catalytic technology. It is envisioned that this review will guide the future development of single-atom photothermal catalysts and significantly advance such an emerging research field.

**Keywords:** Single-atom catalyst, photothermal catalysis, volatile organic compound oxidation, catalyst design, reaction mechanism

## INTRODUCTION

Volatile organic compounds (VOCs) emanating from industrial and routine activities include a spectrum of chemicals, such as benzene, toluene, and formaldehyde<sup>[1,2]</sup>. These substances endanger human health due to their toxicity and contributions to photochemical smog formation upon interaction with atmospheric NO<sub>x</sub>, which aggravates environmental pollution<sup>[3,4]</sup>. These emissions originate from a multitude of sectors, including industrial processes, transportation activities, and solvent usage. The considerable emissions and their significant ecological and health implications have rendered VOCs a pressing environmental concern necessitating mitigation<sup>[5]</sup>. Thus, developing efficacious strategies for VOCs elimination is imperative for air quality enhancement and public health protection.

Thermocatalytic oxidation is an effective method for eliminating VOCs, converting them into less toxic (CO<sub>2</sub> and H<sub>2</sub>O) or high-value organic compounds, thus serving as a beneficial strategy for air quality management<sup>[6-8]</sup>. This process typically operates in a temperature range of 25-500 °C, which is significantly at temperatures lower than *ca.* 800 °C needed for direct thermal incineration<sup>[9]</sup>. However, three common challenges in thermocatalytic oxidation of VOCs are identified: (i) Most of thermocatalytic processes rely on fossil fuels, which are stored in limited quantities, and the heating process leads to substantial CO<sub>2</sub> emissions, limiting energy sustainability and producing undesired greenhouse gases<sup>[10]</sup>; (ii) the balance between thermodynamics and kinetics in catalytic reactions must be considered. Some reactions (e.g., the selective oxidation of VOCs) may require low temperatures for high equilibrium conversions (which are thermodynamically favorable) and high temperatures for high reaction rates (which are kinetically favorable)<sup>[11,12]</sup>; and (iii) catalysts operating at high temperatures over long periods are prone to sintering and deactivation of their structural and active sites<sup>[13]</sup>. To overcome these limitations, there is an urgent need to explore new technologies to reduce reaction temperatures and optimize the energy structure. Photocatalytic oxidation, renowned for its capacity to moderately remove VOCs at room temperature (RT), leverages solar energy (i.e., a naturally abundant, clean, and sustainable alternative)<sup>[14]</sup>. Semiconductor materials such as TiO<sub>2</sub> are commonly used in photocatalysis to generate electron-hole pairs when they are illuminated with specific wavelengths of light. These photogenerated electrons and holes facilitate the reduction of adsorbed oxygen and oxidation of water molecules, yielding the highly reactive radicals (such as O<sub>2</sub><sup>•-</sup> and <sup>•</sup>OH) that can degrade adsorbed pollutants into non-toxic products<sup>[15,16]</sup>. Despite its advantages, photocatalysis encounters three primary challenges<sup>[17,18]</sup>: (i) The narrow light absorption spectrum of conventional photocatalysts, which underutilizes visible (Vis) and infrared (IR) light; (ii) the inefficiency in light absorption and charge carrier transport, leading to low efficiency of photocatalytic VOCs oxidation; and (iii) the limited selectivity of products, due to the different reactivities of specific photogenerated radical species. These challenges hinder the large-scale and industrial application of heterogeneous photocatalytic processes. Photothermocatalysis, an innovative and integrated technology, is applied across a variety of areas, such as CO<sub>2</sub> conversion, water purification, hydrogen production, *etc.*<sup>[19-21]</sup> [Figure 1]. This technology harnesses the synergistic effects of thermal activation and photo-induced reactions to achieve low-energy and high-efficiency VOC elimination and to reduce CO<sub>2</sub> emissions from fossil fuels. Categorized on the basis of the interplay of light and thermal energy, photothermal catalytic oxidation encompasses four types<sup>[22-25]</sup>: photo-driven thermocatalysis, thermally assisted photocatalysis, photo-assisted thermocatalysis, and synergistic photothermocatalysis. Despite the growing interest in photothermal catalysis, its mechanisms remain partially unclear due to its early developmental stage, which has led to some debates.

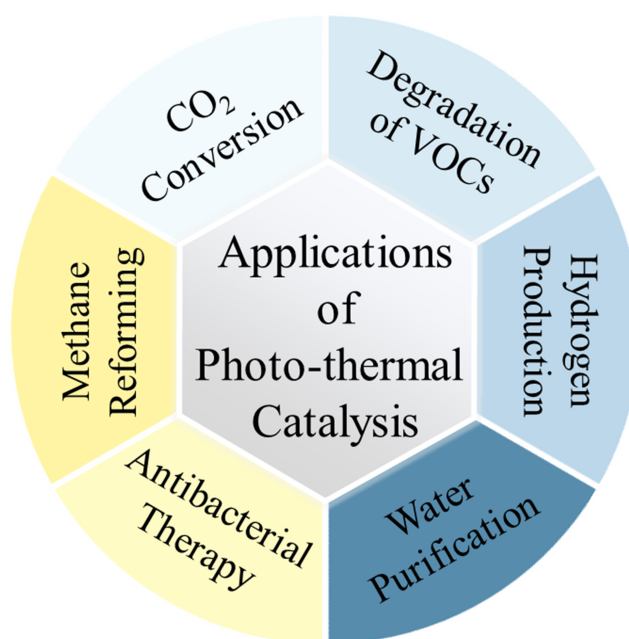


**Figure 1.** Schematic diagram of the main application areas of photothermal catalysis.

As a result, systematic reviews on the fundamental classification and reaction mechanisms of photothermal catalysis are currently lacking.

Developing efficient catalysts is another necessary condition to mitigate VOC pollution and ensure sustainable and green industrial production. In catalytic reactions, the interaction between reactants and catalysts occurs at the active sites, so increasing the proportion of surface atoms of the active component (which is usually an active metal) can directly improve catalytic efficiencies of the catalysts. Reducing the metal active component to the single-atom scale is a catalyst design strategy to maximize the metal utilization. Figure 2 illustrates the schematic diagrams of single-atom catalysts (SACs), single-site heterogeneous catalysts (SSHCs), atomically dispersed supported metal catalysts (ADSMCs), metal nanoclusters, metal nanoparticles (NPs), and metal particle catalysts. SACs can theoretically achieve 100% utilization of metal atoms, which is equivalent to all surface metal atoms being fully exposed<sup>[26]</sup>. The study of isolated metal atoms as active substances in heterogeneous catalysis can be dated back to the pioneering work of Maschmeyer *et al.* in 1995, who reported the formation of an oxygen-coordinated Ti single-atom material for the epoxidation of cycloolefins by grafting metallocene complexes on mesoporous SiO<sub>2</sub><sup>[27]</sup>. In 1999, Asakura *et al.* found that the atomically dispersed Pt species on MgO exhibited a catalytic activity in propane combustion comparable to the metallic Pt particles<sup>[28]</sup>. In 2007, Hackett *et al.* directly observed the atomically dispersed Pd on Al<sub>2</sub>O<sub>3</sub> which showed good catalytic activity in the selective aerobic oxidation of allyl alcohol<sup>[29]</sup>. In 2009, Kwak *et al.* demonstrated that at low Pt loadings ( $\leq 1$  wt%), the atomically dispersed Pt could be anchored on the surface of  $\gamma$ -Al<sub>2</sub>O<sub>3</sub><sup>[30]</sup>. In 2011, Qiao *et al.* dispersed the atomic Pt on an FeO<sub>x</sub> support and first introduced the concept of SACs<sup>[31]</sup>. They prepared a Pt<sub>1</sub>/FeO<sub>x</sub> (Pt loading = 0.17 wt%) catalyst, which exhibited excellent catalytic activity and stability in CO oxidation. Since then, single-atom catalysis has attracted great interest from a number of researchers and has become a new frontier in the catalysis field. Various SAC synthesis strategies have been developed, such as wet chemical methods, photocatalytic reduction, atomic trapping, atomic layer deposition, confinement strategies, and pyrolysis methods. These strategies enable single atoms to form chemical bonds with O, C, N, S, P, *etc.* on the surface of the supports such as oxides, zeolites, carbon, and heteroatom-doped carbon, creating stable catalytic

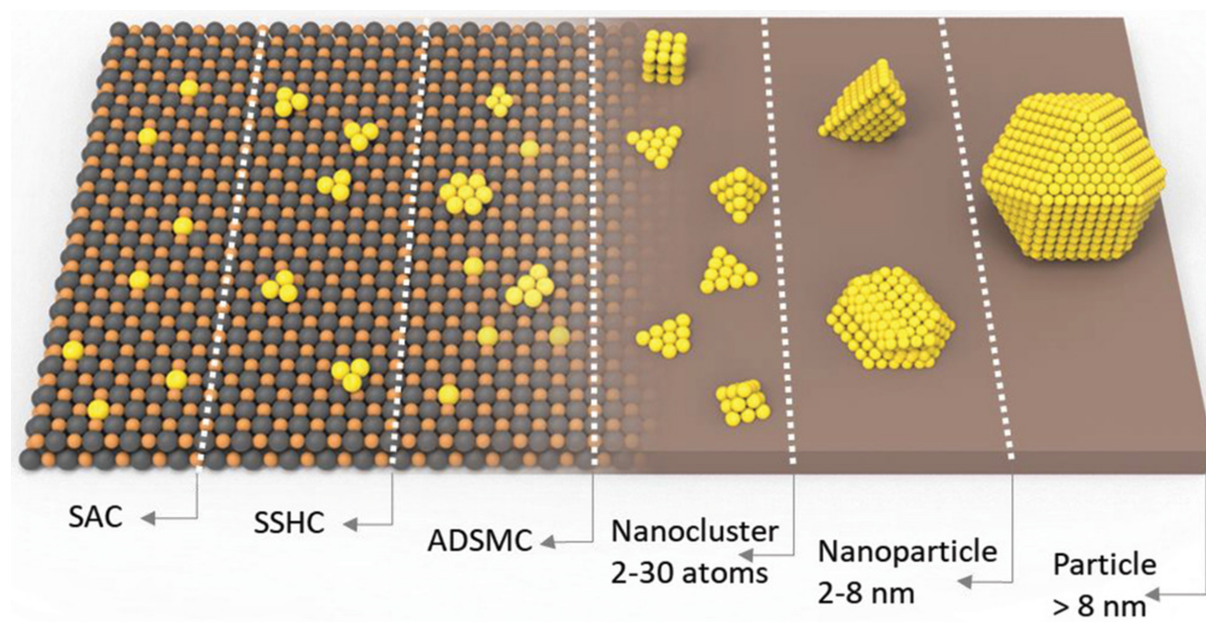


**Figure 2.** Schematic illustration of the various types of SACs, SSHCs, ADSMCs, metal nanoclusters, metal NPs, and metal particles<sup>[26]</sup>. Copyright 2019 Wiley. SACs: Single-atom catalysts; SSHCs: single-site heterogeneous catalysts; ADSMCs: atomically dispersed supported metal catalysts; NPs: nanoparticles.

active sites<sup>[32,33]</sup>. The prepared SACs have shown excellent activity and selectivity in environmentally catalytic reactions, including CO oxidation, NO<sub>x</sub> elimination, VOCs oxidation, CO<sub>2</sub> conversion, and water purification<sup>[34-36]</sup>. Significant progress has been achieved in the SAC investigations, and several high-level reviews have already covered the preparation, characterization, and applications of SACs. Thus, these topics will not be reiterated in this review<sup>[26,32,33,36]</sup>. In recent years, significant advancements have been made in the application research on the SACs in photocatalysis<sup>[37]</sup>, electrocatalysis<sup>[38]</sup>, and thermocatalysis<sup>[39]</sup>. Typically, embedding single atoms into light-absorbing supports alters the band structure and electronic properties, thereby adjusting their light absorption behaviors and charge transfer kinetics<sup>[40]</sup>. Additionally, the low coordination configuration and unsaturated states of SACs facilitate enhanced adsorption and activation of reactant molecules<sup>[41]</sup>. Advanced characterization techniques and important theoretical studies deepen the understanding of SACs, enabling researchers to expect their application potential under different external fields. Beyond the aforementioned applications of SACs, there are many emerging energy conversion fields, such as photothermal and photoelectron catalysis, which are rarely developed using SACs<sup>[42]</sup>. Given the immense potential of SACs, their development with appropriate characteristics can lead to exceptional performance in these applications.

The integration of single-atom catalysis with photothermal catalytic technology marks an emerging research frontier, comprehensive reviews in this area are still limited yet. This review seeks to address the research gap in single-atom photothermal catalysis for VOCs oxidation by analyzing the challenges involved, thus enhancing the academic resources available. Initially, the review categorizes photothermal catalytic systems, emphasizing the mechanisms of photo-driven thermocatalysis and synergistic photothermocatalysis, along with the design principles for efficient photothermal catalysts. Next, it explores the correlation between the structure and performance of SACs in photothermal catalytic VOCs oxidation. Lastly, it conducts a thorough analysis of the potential challenges associated with the SACs in photothermal catalysis for VOCs oxidation, and the future research directions are proposed.



## PHOTOTHERMAL CATALYTIC OXIDATION

In current research, photothermal catalytic oxidation, a technology for VOC elimination that leverages a photo and thermal dual activation mechanism, is recognized for its good efficiency. Photothermal catalysis, as depicted in Figure 3, can be classified into four types based on the roles of photo induction and thermal activation<sup>[43,44]</sup>: (i) Photo-driven thermocatalytic oxidation, where photon energy is converted into thermal energy to reach the ignition temperatures and accelerated the reactions; (ii) thermally assisted photocatalytic oxidation, which boosts the photocatalytic performance by the moderately elevating temperatures; (iii) photo-assisted thermocatalytic oxidation, in which photogenerated charge carriers augment the thermal catalytic pathway, often by modifying the catalyst surface state or promoting the intermediate steps; and (iv) synergistic photothermocatalytic oxidation, which integrates the effects of photocatalysis and thermocatalysis, modulates reaction pathways and products selectivities by interfacing the catalyst surface reactivity with photocatalytic processes<sup>[22-25]</sup>.

Nevertheless, characterizing these reactions poses challenges due to the need for sophisticated measurement techniques to assess local heating and charge transfer, and to quantify the contributions of light and heat in catalytic oxidation<sup>[45]</sup>. Researchers primarily investigate VOCs oxidation within the framework of photo-driven thermocatalysis and photothermocatalysis. Photothermocatalysis generally includes photo-assisted thermocatalysis, thermally assisted photocatalysis, and synergistic photothermocatalysis. Figure 4 illustrates the common photo-driven thermocatalytic device and synergistic photothermocatalytic device utilized in the catalytic oxidation of VOCs.

### Photo-driven thermocatalytic oxidation

Enhancing the energy of reactant molecules and accelerating intermolecular collisions to promote the breaking of bonds in reactants and formation of products on the catalyst surface are crucial for increasing the catalytic reaction rates. This is particularly evident in the thermocatalytic oxidation of VOCs, where heat input is indispensable. Photo-driven thermocatalytic processes keep the principles of traditional thermocatalysis, utilizing the photo-derived heat to overcome the activation energy of reaction and substitute for fossil fuels<sup>[46]</sup>. Here, photocatalytic performance of the catalyst is less pronounced, imposing high demands on the photothermal conversion efficiency of catalytic materials and posing challenges.

#### *Photothermal conversion mechanism*

The photothermal effect in catalytic VOCs oxidation is the process where catalytic materials convert light energy directly into thermal energy, a phenomenon found in both inorganic (e.g., noble metals and semiconductors) and organic [e.g., carbon-based materials and metal-organic frameworks (MOFs)] catalysts. This effect is mainly due to the localized surface plasmon resonance (LSPR), non-radiative relaxation in semiconductors, and molecular thermal vibrations<sup>[47]</sup>. The characteristics of these materials dictate the pathways for converting light energy into heat, which can involve either a single mechanism or the combined action of several mechanisms. In metallic materials, the LSPR arises when frequency aligns of photon with the natural frequency of the electrons on the metal surface, inducing the coherent oscillations via the charge-photon resonance. Upon irradiation at their resonant wavelengths, metal NPs experience the plasmon-assisted photothermal effects, which generate hot electrons<sup>[48,49]</sup>. These electrons decay either via the radiative emission or the carrier multiplication triggered by the electron-electron interactions. The scattering process redistributes the energy of hot electrons, causing a swift rise in the local surface temperature of the metal. Subsequently, the energy transfer from electrons to lattice phonons initiates the equilibrium cooling. Phonon-phonon coupling within the lattice facilitates cooling and the dissipation of heat into the surrounding medium, thereby elevating the local temperature<sup>[50,51]</sup> [Figure 5A]. In semiconductor materials, the electrons excited by light transition to higher energy states then return to the

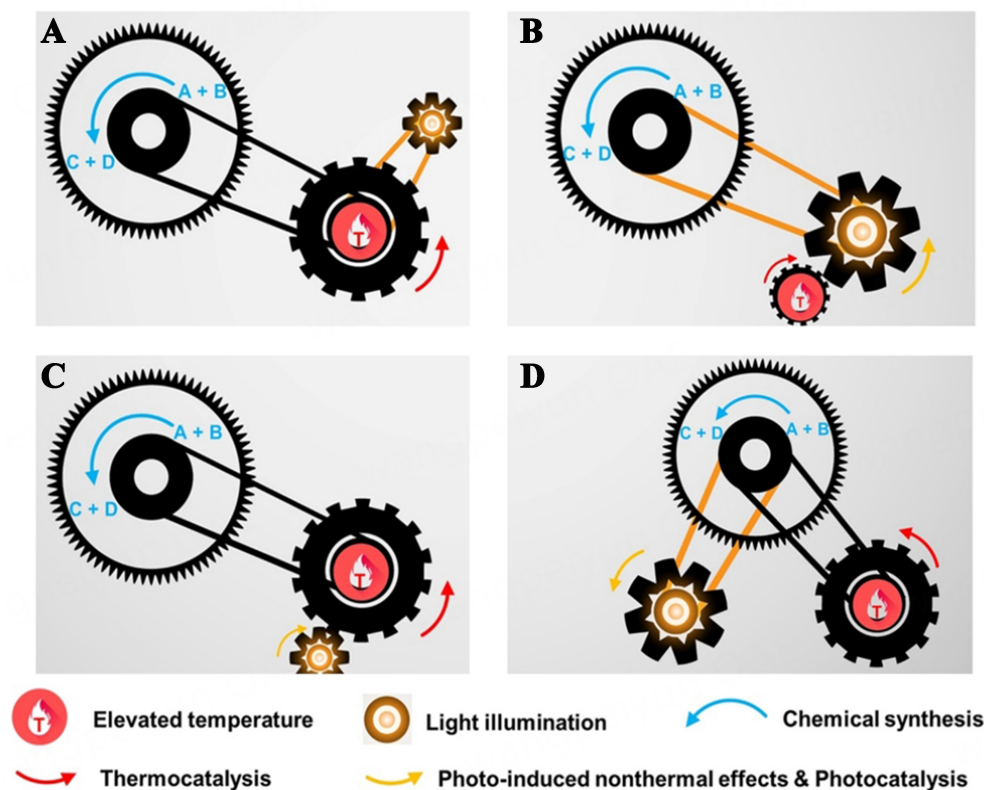


**Figure 3.** Schematic illustration of four discrete categories of photothermocatalysis. (A) Photo-driven thermocatalysis; (B) Thermally assisted photocatalysis; (C) Photo-assisted thermocatalysis; and (D) Synergistic photothermocatalysis<sup>[43]</sup>. Copyright 2023 Cell Press.

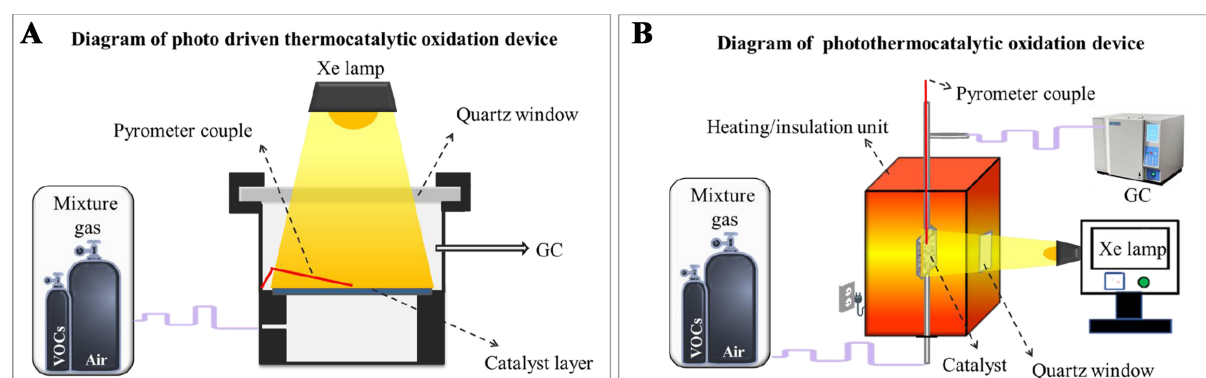


**Figure 4.** Diagrams of common catalytic oxidation of VOCs. (A) Photo-driven thermocatalytic device; and (B) Synergistic photothermocatalytic device. VOCs: Volatile organic compounds.

lower ones. This transition releases energy, which is transferred to impurities/defects or surface dangling bonds via either the radiative relaxation (as photons) or non-radiative relaxation (as phonons)<sup>[52,53]</sup>. The release of energy in the form of phonons results in the localized lattice heating. In carbon-based materials, photothermal conversion involves the electron transitions from lower to higher orbital states, exciting electrons from the valence band (VB) to the conduction band (CB). These excited electrons relax via the electron-phonon coupling, transferring the absorbed light energy to the vibrational modes of the entire atomic lattice and increasing the macroscopic temperature of the material<sup>[54,55]</sup>. Organic nanomaterials share

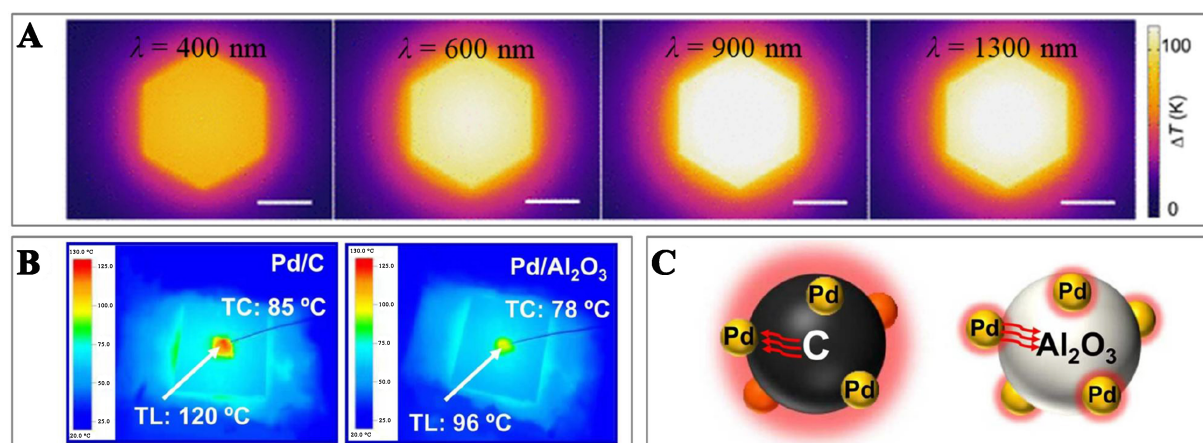


**Figure 5.** (A) The spatial distribution of the temperature rise due to photothermal effects on a Pd nanosheet at different wavelengths of light (at a power density of  $1 \text{ mW} \cdot \mu\text{m}^{-2}$ )<sup>[49]</sup>. Copyright 2024 American Association for the Advancement of Science; (B) IR image over the Pd/C, and Pd/Al<sub>2</sub>O<sub>3</sub> catalysts with light irradiation of  $200 \text{ mW} \cdot \text{cm}^{-2}$ ; and (C) Heat transfer mechanism over the Pd/C and Pd/Al<sub>2</sub>O<sub>3</sub> catalysts<sup>[57]</sup>. Copyright 2022 Elsevier. IR: Infrared.

a photothermal conversion mechanism similar to that of carbon-based materials. Upon illumination,  $\pi$ - $\pi^*$  transitions occur in the benzene rings, reducing the band gap between the VB and the CB<sup>[56]</sup>. This facilitates the charge transfer, driving lattice vibrations and increasing the temperature of the organic molecular material. The composition of a photothermal catalyst enables two or more interactive mechanisms that result in the localized surface heating<sup>[57]</sup>, as depicted in Figure 5B and C.

Photothermal conversion efficiency ( $\eta$ ), a critical parameter for evaluating the performance of a photo-derived thermocatalytic material, is often overlooked in research. It is defined as the ratio of the thermal energy converted by the material to the incident light energy, as calculated by

$$\eta = \frac{E_{\text{thermal}}}{E_{\text{photons}}} \times 100\%$$

where  $E_{\text{photons}}$  represents the incident light energy from irradiation, while  $E_{\text{thermal}}$  denotes the thermal energy converted on the catalyst surface. The pertinent studies offer a comprehensive explanation of the detailed calculation formulas<sup>[58,59]</sup>. Some studies showed that the CeO<sub>2</sub>/LaMnO<sub>3</sub> composite had a broad light absorption range of 800–1,800 nm. This material served as a highly active catalyst for VOC decomposition under IR irradiation. At an IR irradiation intensity of  $280 \text{ mW} \cdot \text{cm}^{-2}$ , its maximum photothermal conversion efficiency reached 15.2%<sup>[60]</sup>. In the photo-driven thermocatalytic decomposition of formic acid to produce pure CO using a fluorite-type ZrO<sub>2</sub> system, the ZrO<sub>2</sub> nanosheets achieved a photothermal energy conversion efficiency of 12.3% at an IR irradiation intensity of  $500 \text{ mW} \cdot \text{cm}^{-2}$ <sup>[61]</sup>. In the photo-driven thermocatalytic CO<sub>2</sub>-methane dry reforming reaction, the Ni NPs were loaded on the silicate nanotubes and coated with a layer of CeO<sub>2</sub> to form a novel encapsulated photothermal catalyst (Ni-psnts@CeO<sub>2</sub>). This material achieved a photothermal conversion efficiency of 36.9%<sup>[62]</sup>. In practical applications, however, the photothermal conversion efficiency is influenced by various factors, including the catalyst, reaction condition, and light intensity.

#### Design of photo-driven thermocatalysts

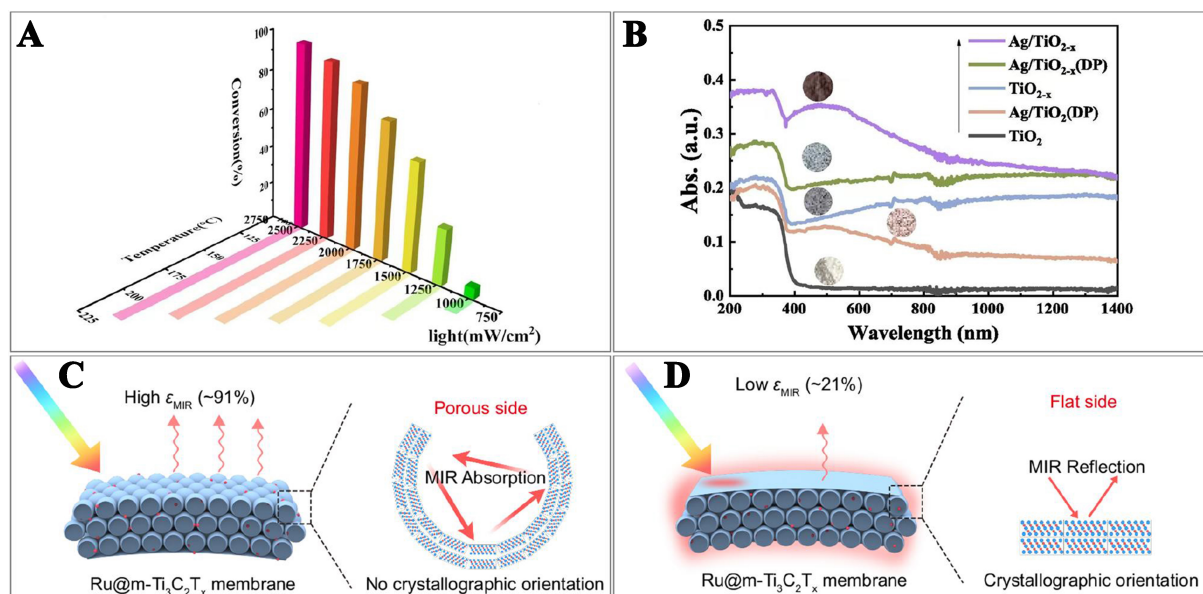
In catalyst design, several key factors should be considered to enhance photo-derived thermocatalysis performance, such as improving light absorption, optimizing internal electric fields for high-energy thermal electrons and localized thermal effects, constructing active sites, and managing thermal energy storage.

Figure 6A depicts the correlation of light power density or catalyst temperature to VOC conversion<sup>[63]</sup>. The catalyst design aims to achieve optimal performance, i.e., trying to achieve a good effect that the surface reaches a temperature adequate for catalyzing VOC elimination under natural sunlight illumination. Efficient light absorption is fundamental to this catalytic process. Dark-colored catalysts are chosen for their ability to absorb photons effectively, converting light into thermal energy and minimizing both re-radiation and energy loss to non-thermal forms, which rapidly increases the catalyst surface temperature and activates thermocatalytic reactions. For instance, the molecular dispersion of cobalt phthalocyanine (CoPc) on carbon nanotubes (CNTs) enabled the efficient conduction of photo-derived thermocatalysis. Research indicated that CNTs not only facilitated the anchoring and dispersion of CoPc molecules (providing the active and stable catalytic sites), but also converted solar energy into localized heat (promoting the reactions at optimal temperatures)<sup>[64]</sup>. Zhang *et al.* demonstrated that surface site engineering could convert pale yellow and non-photothermally active  $\text{In}_2\text{O}_3$  NPs into black and photothermally active  $\text{H}_x\text{In}_2\text{O}_{3-x}(\text{OH})_y$ <sup>[65]</sup>. In addition, adjusting the bandgap of a semiconductor to optimize the full-spectrum solar light absorption and enhance the photothermal conversion is a proven method for improving catalytic performance, such as the commonly used doping (which can create defect sites) and constructing heterostructures<sup>[66]</sup>. For instance, Fang *et al.* employed a one-step solid-state calcination and reduction method to introduce surface defects and load Ag NPs on the surface of  $\text{TiO}_2$ . The resulting black Ag/ $\text{TiO}_{2-x}$ , characterized by a high concentration of surface vacancies and a narrow bandgap, responded to the full solar spectrum and possessed an enhanced light absorption via the LSPR effect of Ag NPs [Figure 6B], leading to the significant improvement in toluene oxidation rate<sup>[67]</sup>. Defective  $\text{Mn}_3\text{O}_4$  could harness solar energy for the photo-derived thermocatalytic oxidation of ethyl acetate, eliminating the need for additional energy input. By reducing the coordination numbers of Mn–O and Mn–Mn bonds, the bandgap structure was adjusted, enhancing light absorption and leading to efficient catalytic oxidation under natural light irradiation<sup>[68]</sup>. Noble metal NPs with a LSPR effect supply a heat source for the catalyst. Meanwhile, these catalysts, known for their superior catalytic performance (i.e., reducing activation energy, facilitating chemical bond cleavage, and optimizing the adsorption and desorption of reactants and intermediates), are extensively applied in the photothermal catalytic oxidation of VOCs. For example, Elimian *et al.* employed molecular sieves with high specific surface areas to disperse oxygen vacancy-rich  $\text{TiO}_2$  and Pt NPs, combining light absorption and catalytic activity to swiftly convert light energy into thermal energy, thereby driving the photothermal catalytic oxidation of toluene<sup>[69]</sup>. In addition to these developments, various thermal insulation materials have been engineered to address specific heat loss mechanisms. These materials include the  $\text{SiO}_2$  insulation layers, the MOFs with imidazolium esters, the Cu coatings that mitigate IR radiation, and the innovative polyethylene glycol (PEG)/MXene material for thermal energy storage<sup>[70]</sup>. Liu *et al.* employed the physical vapor deposition method to sequentially deposit a Ti/Al/ $\text{SiO}_2$ / $\text{SiO}_2$ -Ni multilayer structure on a polyimide (PI) film. This approach reduced energy loss from thermal radiation and consequently significantly enhanced the photothermal temperature on the catalyst surface<sup>[71]</sup>. Moreover, a catalyst comprising hollow  $\text{Ti}_3\text{C}_2\text{T}_x$  spheres loaded with Ru NPs and encapsulated by overlapping planar  $\text{Ti}_3\text{C}_2\text{T}_x$  flake layers was designed to minimize the thermal radiation, maximize the solar light absorption, and preserve the catalytic activity, resulting in superior catalytic performance<sup>[72]</sup> [Figure 6C and D].

#### Limitations of photo-driven thermocatalytic VOCs oxidation

(i) Reactor design imperfections compromise the test accuracy. In photo-driven thermocatalytic lab tests, the catalyst surface temperature is completely determined by the illumination. Thermocouples, typically positioned at the catalyst layer center, record higher temperatures than those at the edges. This discrepancy in test hampers accurate determination of the catalyst surface temperature.





**Figure 6.** (A) Correlation among light power density, catalyst temperature, and VOCs conversion<sup>[63]</sup>. Copyright 2024 Elsevier; (B) Solid UV-Vis-IR diffuse reflectance spectra of  $\text{TiO}_2$ ,  $\text{TiO}_{2-x}$  and  $\text{Ag/TiO}_{2-x}$ <sup>[67]</sup>. Copyright 2024 Elsevier; Schematic of (C) low photothermal effect of the porous side without planar  $\text{Ti}_3\text{C}_2\text{T}_x$  flake layers and (D) high photothermal effect of the flat side with planar  $\text{Ti}_3\text{C}_2\text{T}_x$  flake layers. The  $\epsilon_{\text{MIR}}$  means minimized thermal emission (mid-IR emissivity)<sup>[72]</sup>. Copyright 2024 Springer Nature. VOCs: Volatile organic compounds; UV-Vis: ultraviolet-visible; IR: infrared.

(ii) Certain limitations are encountered in practical applications. To achieve high reactant conversions over the catalysts, high-intensity illumination is required (several to tens of solar intensity), which poses difficulty for directly using solar energy to completely oxidize VOCs. The proposed current method, which uses a convex lens to focus light to natural intensity, is constrained by the reactor size limitation. In practical working conditions, cloudy or dark environments can halt the photo-driven thermocatalytic reaction, thereby restricting its industrialization. Therefore, constructing a catalytic capable of autonomous operation without sunlight is equally important<sup>[73]</sup>.

### Photothermocatalytic oxidation

Photoexcited catalysts can induce thermal and non-thermal effects as shown in Figure 7, with the latter also playing a significant role in promoting chemical reactions, a fact that should not be overlooked<sup>[43]</sup>. The primary non-thermal chemical effects in supported catalysts induced by photoexcitation include: (i) The modulation of reactant adsorption by the photogenerated charge carriers<sup>[74]</sup>; (ii) the promotion of surface catalytic redox reactions via the charge carriers consumption<sup>[75]</sup>; and (iii) the regulation of the catalyst surface state<sup>[76]</sup>. The photothermocatalytic effect, resulting from the synergistic interaction between thermal activation and photo-induced pathways, markedly enhances the catalytic activity and allows for the regulation of reaction pathways and product selectivities<sup>[77]</sup>. Research methods are primarily divided based on the dominant catalytic mechanisms: one approach introduces a heat source into the photocatalytic system, while the other integrates a light source into the thermal catalytic system. Distinguishing between these two interwoven catalytic pathways in the photothermocatalytic process is often challenging.

### Thermal-assisted photocatalytic oxidation

The thermally assisted photocatalysis depends largely upon the light-driven reactions, with the catalyst having minimal thermocatalytic activity. This process mainly involves the photogenerated carriers of the catalyst. Temperature usually plays a dual role in traditional gas-solid phase catalysis: It can reduce the

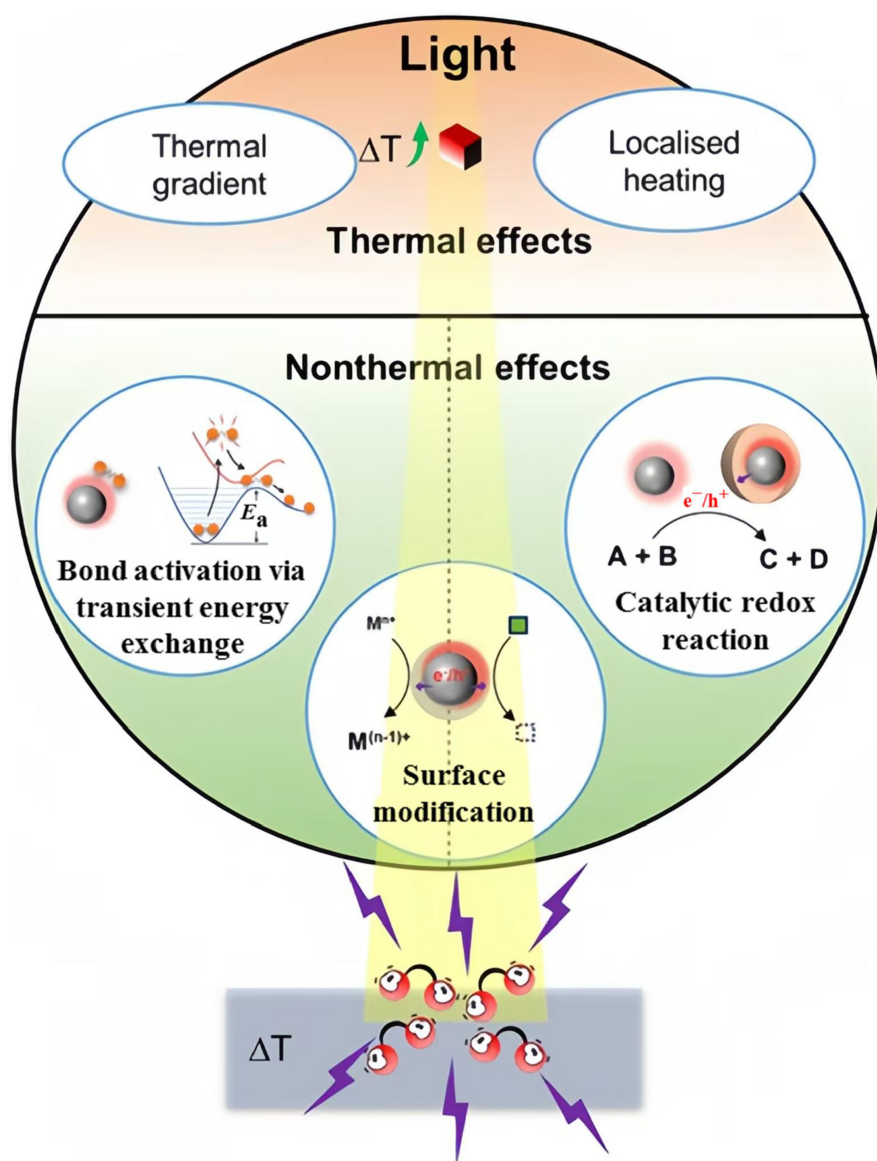


**Figure 7.** Schematic diagram of thermal and non-thermal effects in the photothermocatalysis<sup>[43]</sup>. Copyright 2023 Cell Press.

apparent activation energy of photocatalysis, thus enhancing the mobility of photogenerated charge carriers and mass transfer efficiency of the reactants<sup>[78,79]</sup>, but it may also lead to rapid recombination of charge carriers and disruption of reactants adsorption<sup>[74]</sup>. For instance, as a typical photocatalyst,  $\text{TiO}_2$  exhibits significant activity in degrading VOCs under the ultraviolet (UV)-Vis light illumination. During the photocatalytic removal of benzene, toluene, and xylene, VOC adsorption on  $\text{TiO}_2$  facilitated the formation of interfacial complexes. The initial photo-oxidation of toluene to benzaldehyde on  $\text{TiO}_2$  was activated by these complexes under the Vis light illumination, and benzaldehyde was further oxidized to  $\text{CO}_2$  with additional thermal energy. This synergistic effect of photo and thermal energy boosted photothermal catalysis, hastening the complete oxidation of toluene into  $\text{CO}_2$ <sup>[80]</sup>. The {103} facet of  $\text{Mn}_3\text{O}_4$  was reported to be of a superior photothermal catalytic activity, enabling the complete oxidation of HCHO at RT. The HCHO conversion over the  $\text{Mn}_3\text{O}_4$  catalyst in thermocatalysis alone at 48 °C was only 11%. When the photocatalytic temperature dropped from 25 to 5 °C, the formaldehyde conversion reduced from 71% to

27%, underscoring the significance of thermally assisted photocatalysis in the photothermal mechanism [Figure 8A]. The {103} facet of  $\text{Mn}_3\text{O}_4$  displayed the optimal photothermocatalytic activity due to enhanced absorption of UV-Vis light and more efficient separation of the photogenerated electron-hole pairs<sup>[81]</sup>.

#### *Photo-assisted thermocatalytic oxidation*

In photo-assisted thermocatalytic reactions, thermal energy is the primary driver. Figure 8B depicts that under the Vis light irradiation,  $\text{PdO}/\text{Mn}_3\text{O}_4/\text{CeO}_2$ <sup>[82]</sup> significantly reduces the temperatures required for 10% ( $T_{10\%}$ ) and 50% ( $T_{50\%}$ )  $\text{CH}_4$  conversions to 180 and 225 °C, respectively. Moreover, light irradiation was found to substantially enhance the thermocatalytic efficiency at constant reaction temperatures, a phenomenon that was clearly demonstrated in Figure 8C. Light irradiation may excite molecular vibrations by increasing the local temperature, thereby inducing a photothermal effect<sup>[83]</sup>, while the photochemical effect also plays a significant role in the reaction<sup>[84]</sup>. Investigating how the photogenerated charge carriers influence or alter surface chemistry and electronic properties of the catalysts and intermediate reaction steps has become a central issue<sup>[85,86]</sup>. A thorough analysis of electron transfer pathways and their impact on the catalyst surface states and adsorption behaviors is of decisive significance for elucidating the photothermocatalytic activity and the overall reaction mechanism. Under the assistance of the simulated sunlight, the *p-n* heterojunction formed in  $\text{Co}_3\text{O}_4/\text{TiO}_2$  exhibited a superior photothermocatalytic activity towards toluene oxidation. Within the *p-n* heterojunction [ $\text{MO}_x/\text{TiO}_2$  ( $M = \text{Co}, \text{Mn}, \text{Ce}, \text{Cu}, \text{Fe}$ )] composed of different semiconductors, the effective separation of electrons and holes generated an interfacial potential difference, which not only suppressed the recombination of electron-hole pairs but also enhanced the quantum yield and generated more active free radicals. These radicals played a key role in the complete oxidation of toluene. Upon photoexcitation, the active charge carriers produced by the catalyst directly participated in the reaction, and these carriers could also transfer to the unoccupied molecular orbitals of adsorbed molecules, initiating the photochemical reactions. Consequently, in catalytic reactions where thermal energy was the primary driving force, the active species introduced by photoactivation effectively reduced the temperature required for the reaction and accelerated the oxidation process of toluene and its intermediates<sup>[87]</sup>.

#### *Synergistic photothermocatalytic oxidation*

The synergistic photothermocatalytic system propelled by the dual photothermic activation can harness a synergistic effect of thermal activation and photo-induced reactions. The heat for photothermic effects accelerates reaction kinetics, and the photochemical effect notably enhances apparent activity, surpassing the sum of individual thermo- and photocatalysis. This synergism results in a good catalytic activity that exceeds the combined activities of separate photo and thermal catalytic processes, leading to marked improvements in catalytic activity and/or selectivity<sup>[88]</sup>. In the synergistic photothermocatalytic oxidation of toluene, the results reported in the literature indicated that benzoic acid accumulated significantly under the thermocatalysis alone condition. In contrast, the synergistic thermo- and photoactivation effectively surmounted the energy barrier to benzoic acid ring-opening, further oxidizing it to maleic anhydride, thus achieving the complete oxidation of toluene<sup>[89]</sup>. Additionally, it was found that there was an interaction between the reactive oxygen species generated by photocatalysis (such as hydroxyl and superoxide radicals) and the carboxylic acids produced by thermocatalysis. Photocatalysis facilitated the formation of aldehydes and the consumption of carboxylic acids, whereas thermocatalysis accelerated the accumulation of carboxylic acids and the degradation of aldehydes. This interaction significantly enhanced the oxidation process of toluene<sup>[90]</sup>. Given the presence of the synergistic photothermocatalytic effect, studying and regulating the impact of individual stimuli (light or heat) and surface processes on the catalysts present a challenging task. Currently, the strategies for enhancing the performance of synergistic photothermocatalysts primarily involve the construction of heterostructures, bimetallic NPs, and surface defects, with the aim of strengthening the combined performance of photo- and thermocatalysis<sup>[91]</sup>. The

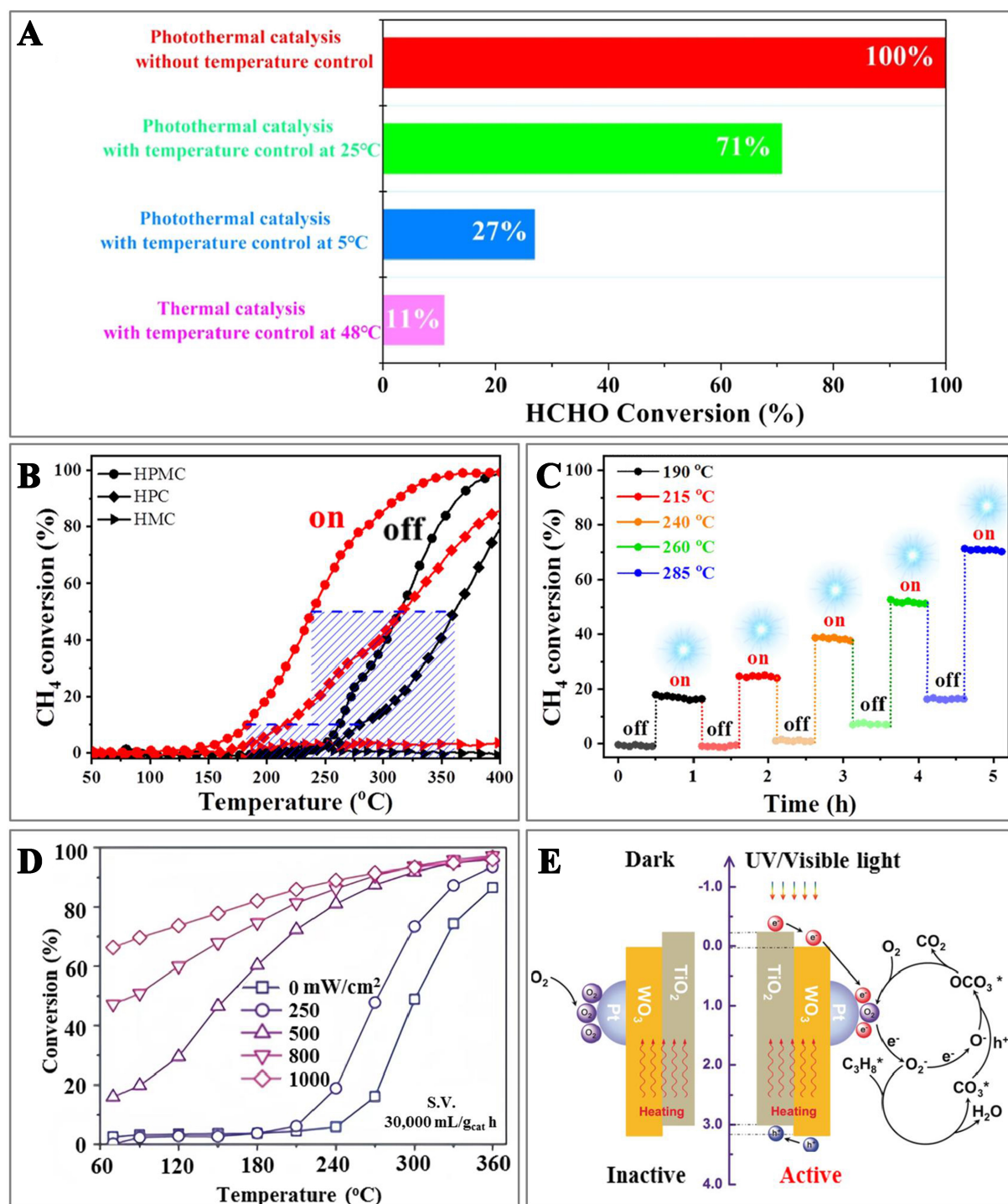


**Figure 8.** (A) Photothermal- or thermocatalytic activity over the catalyst under the controlled reaction conditions<sup>[81]</sup>. Copyright 2023 American Chemical Society; (B) Conversion curves and (C) cycling stability test with or without irradiation (on/off)<sup>[82]</sup>. Copyright 2021 Wiley; (D) Catalytic activity over the catalyst under the light illumination with different power density in synergistic photothermocatalytic oxidation; and (E) Comparison of possible reaction mechanisms of thermocatalytic and photothermocatalytic oxidation of C<sub>3</sub>H<sub>8</sub><sup>[94]</sup>. Copyright 2020 Wiley.

construction of heterostructures encompasses the formation of heterojunctions between noble metal NPs and semiconductors<sup>[92]</sup> and the enhancement of electron transfer via multiple heterointerfaces<sup>[93]</sup>. For



example, the Pt/TiO<sub>2</sub>-WO<sub>3</sub> catalyst showed a notable activity increase in the photothermocatalytic oxidation of propane<sup>[94]</sup>. Under the UV-Vis light irradiation, the reaction temperature for a propane conversion of 70% reduced significantly from 324 to 90 °C [Figure 8D], and the apparent activation energy decreased from 130 to 11 kJ·mol<sup>-1</sup>. The construction of heterostructures facilitated the effective charge separation, leading to the efficient generation of oxidative free radicals. Concurrently, the conductivity of semiconductors increases exponentially with temperature, suggesting that higher temperatures may aid in transferring the more high-energy charge carriers to the active sites of the catalyst. From a thermocatalytic perspective, heating also favors the desorption and transformation of intermediates on the catalyst surface [Figure 8E]. Altering the composition of bimetallic NPs regulates their surface electronic structures and geometries, thereby modulating the adsorption properties of reactants and products. This modulation enables the precise control on the catalytic activity, selectivity, and stability, offering another effective method for the optimization of catalytic performance<sup>[95,96]</sup>. Defect engineering strategies effectively enhance light absorption efficiency and charge separation by strengthening the surface active sites and modulating the band structures<sup>[97]</sup>. For instance, the controlled synthesis of Mn<sub>3</sub>O<sub>4</sub>-based catalysts with unsaturated coordination defects exhibited excellent synergistic photothermocatalytic performance in the oxidation of ethyl acetate and other OVOCs under simulated sunlight or even natural light illumination. Research results revealed that light irradiation influenced the migration of lattice oxygen and initiated the C-H bond cleavage of the CH<sub>3</sub>CH<sub>2</sub>• in ethyl acetate dissociation. Concurrently, the formation of oxygen vacancies played a crucial role in enhancing the activation and dissociation of O<sub>2</sub>, which was then transformed into the highly reactive oxygen species that participated in the deep oxidation process on the catalyst surface<sup>[68]</sup>.

#### *Limitations of photothermocatalytic VOCs oxidation*

(i) Measuring reaction temperatures in photothermocatalytic processes poses a challenge as well. Thermocouples are used to determine the oxidation temperatures of VOCs by measuring only the outer surface temperatures of the catalysts. However, they cannot precisely capture the localized temperature changes caused by the conversion of photons, which introduces inaccuracies in the thermodynamic and kinetic analysis of photothermocatalysis.

(ii) There is no consensus on the mechanism of photothermocatalysis. Researchers typically analyze catalytic mechanisms from photo- or thermocatalytic perspectives. However, the use of *in situ* analysis techniques is limited, and detecting transient species is challenging. Despite the broad application of density functional theory (DFT)-based calculations in catalytic reaction studies and predictions, the numerous intermediate products in photothermocatalytic processes necessitate greater precision in theoretical calculations.

## **SINGLE-ATOM PHOTOTHERMAL CATALYSIS**

### **Advantages of SACs**

Strictly speaking, SACs expose all of the catalytically active metal atoms on the surface of a catalyst, achieving 100% atomic utilization. This feature is particularly attractive for reducing the cost of noble metal-based catalysts. Additionally, SACs bridge homogeneous and heterogeneous catalysis. Given the outstanding performance and potential applications of SACs in photo- and thermo-catalysis, the future looks promising for the photothermal catalytic oxidation of VOCs.

#### *Single-atom photocatalytic oxidation*

In photocatalytic reactions, three key steps are involved: light absorption, charge carriers generation and separation, and catalytic reaction. Firstly, narrowing the bandgap within a specific range is crucial for generating the photogenerated electron-hole pairs. Embedding single atoms in the support modifies its

band structure. The CB and VB positions of a photocatalyst must align with the redox potentials of the reaction to initiate the photocatalytic process<sup>[98]</sup> [Figure 9A]. At the same time, this modification also broadens the light response range and enhances light absorption. Secondly, the migration of photogenerated carriers from the photocatalyst surface to the reactant molecules is essential for the redox reaction. Studies indicate that introducing single atoms on semiconductors can accelerate the transfer of the photogenerated electron-hole pairs, thereby speeding up the catalytic reaction<sup>[99]</sup>. As shown in Figure 9B, the Schottky barrier between metal NPs and support typically hinders the extraction of the photoexcited electrons, thereby reducing electron transfer and injection efficiency. However, when the size of metal NPs is reduced to single atoms, their unique coordination structure with the support can significantly enhance the metal-support interaction, thus accelerating electron transfer<sup>[100]</sup>. Thirdly, the adsorption and activation of reactants on the SAC catalysts are essential for catalytic reactions. By adjusting the coordinately unsaturated single-atom active sites, more favorable conditions and pathways for reactants and intermediates adsorption and activation on the catalyst surface can be created [Figure 9C]. In the photocatalytic VOCs oxidation, the single-atom catalytic process is relatively straightforward, traceable to the initial activation steps, which include the photoexcited carrier separation and transfer, molecular adsorption, intermediate formation, and final product desorption<sup>[101]</sup>.

#### *Single-atom thermocatalytic oxidation*

The SACs demonstrate high uniformity in geometric configuration, coordination environment, and electronic state. This uniformity significantly modulates the selectivity and activity of thermocatalytic VOCs oxidation via electronic and steric effects<sup>[41]</sup>. Adjusting the coordination environment of SACs can alter the adsorption/desorption selectivity and adsorption strength of the active components towards different molecules, thereby affecting the catalytic activity and stability<sup>[102,103]</sup>. For example, reducing the oxygen coordination number of Pt atoms through the reduction treatment adjusted the adsorption strength of toluene, leading to the efficient and stable elimination of VOCs<sup>[104]</sup> [Figure 9D]. The precise metal single-atom acts as the active site, which simplifies the determination of reaction mechanisms and provides an ideal platform for studying the structure-activity relationship at the atomic scale. The SACs that obey the Mars-van Krevelen (MvK) mechanism typically react by activating the surface lattice oxygen species. This mechanism is prevalent in the catalytic oxidation of hydrocarbons over the SACs supported on reducible metal oxides<sup>[105]</sup>. Introducing single-atom enhances catalytic activity of VOCs oxidation by creating surface oxygen vacancies and boosting the reactivity of surface lattice oxygen, which reduces the reaction activation energy<sup>[106]</sup>. The Langmuir-Hinshelwood (L-H) mechanism is a prevalent process in thermocatalytic reactions. It involves the adsorption of reactant molecules on the catalyst surface, followed by the interactions between these adsorbed reactants. The SACs reduce the activation energy for reactions between VOCs and O<sub>2</sub>, thus altering the reaction pathways. This mechanism is commonly observed in the reactions such as catalytic hydrocarbon conversions and CO oxidation<sup>[107]</sup>, as shown in Figure 9E. The Eley-Rideal (E-R) mechanism involves one reactant in the gas phase and another reactant adsorbed on the catalyst surface. In the VOCs oxidation, the SACs effectively activate oxygen molecules, generating the highly reactive oxygen species<sup>[108]</sup>. These species serve as key intermediates in the E-R mechanism, directly reacting with VOCs molecules<sup>[109]</sup> [Figure 9F]. Typically, the thermocatalytic VOCs oxidation mechanism over the SACs depends upon various conditions, such as the type of the metal atom, the nature of the support, and the temperature of the reaction. In addition, for the single-atom thermocatalysts, the thermal stress during reactions may lead to their deactivation, causing single atoms to aggregate and form the low active clusters. The SACs are also susceptible to high-temperature sintering, which results in losing of their unique properties of single atoms and formation of the particles. This issue is crucial in high-temperature oxidation reactions. To mitigate this phenomenon, the catalyst preparation methods including high-temperature pyrolysis, impregnation/co-precipitation calcination, high-temperature thermal migration, and heteroatom doping can effectively prevent single-atom sintering<sup>[110,111]</sup>. High-temperature pyrolysis decomposes metal

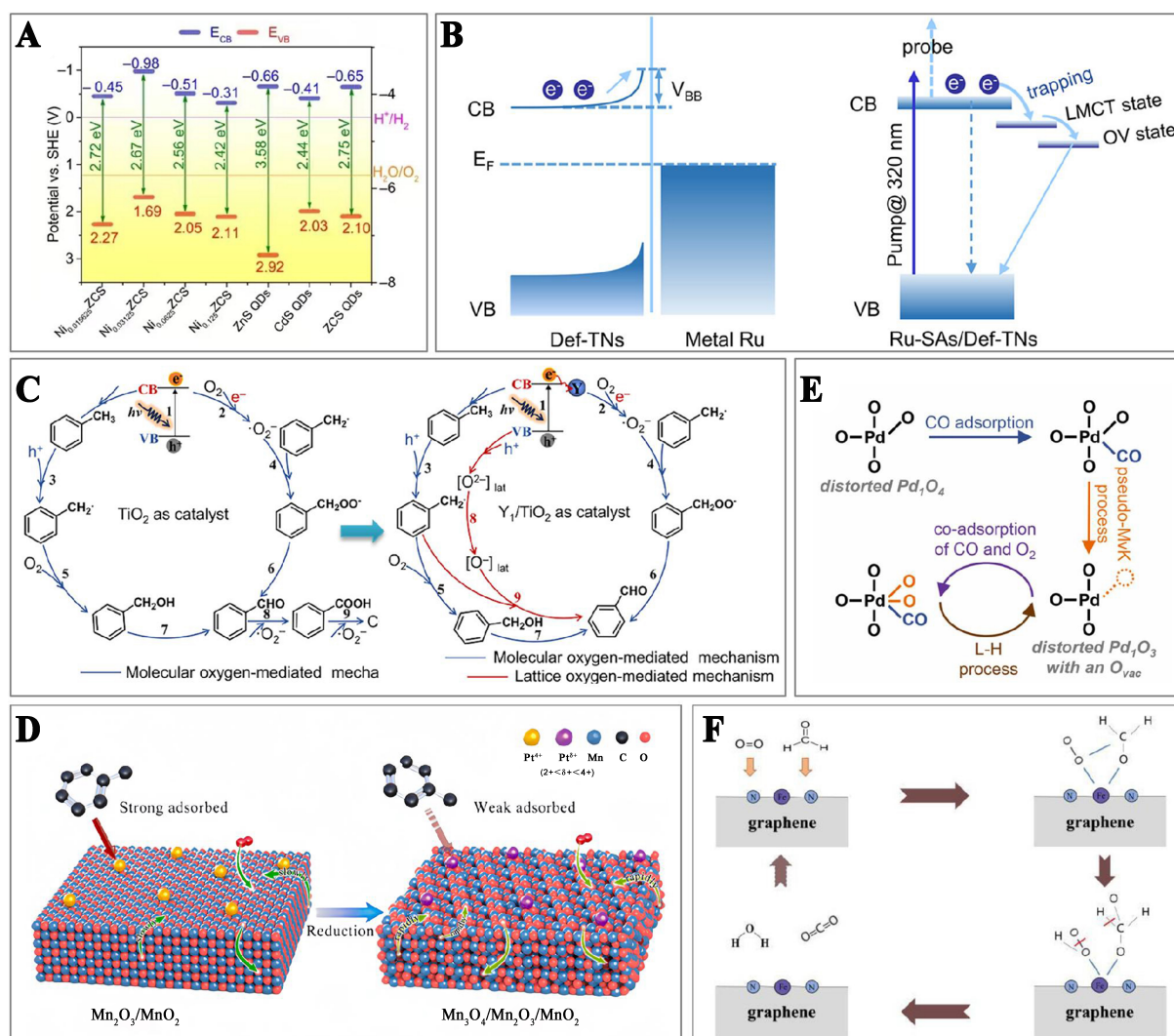


**Figure 9.** Single-atom photocatalysis: (A) Band alignments for Ni single-atom decorated zincblende cadmium-zinc sulfide quantum dots and control samples<sup>[98]</sup>. Copyright 2020 American Association for the Advancement of Science; (B) Mechanisms underlying the photoexcited electron dynamics involved in Ru NPs and Ru single-atom based catalyst<sup>[100]</sup>. Copyright 2020 American Chemical Society; (C) Possible process of selective photocatalysis of toluene oxidation over the catalysts with pure support and single-atom introduction<sup>[101]</sup>. Copyright 2024 American Chemical Society. Single-atom thermocatalysis: (D) Schematic illustration of the enhancement in catalytic stability for toluene removal over the supported Pt SACs with the regulated coordination environments<sup>[104]</sup>. Copyright 2021 Elsevier; (E) Schematic diagram of MvK and L-H mechanism over the Pd SACs<sup>[107]</sup>. Copyright 2023 Elsevier; (F) Schematic diagram of E-R mechanism of catalytic HCHO oxidation over the Fe SACs<sup>[109]</sup>. Copyright 2022 Elsevier. NPs: Nanoparticles; SACs: single-atom catalysts; MvK: Mars-van Krevelen; L-H: Langmuir-Hinshelwood; E-R: Eley-Rideal.

precursors at high temperatures, allowing metal atoms to coordinate with heteroatoms in the support, thereby preventing sintering. Impregnation/co-precipitation followed by calcination constructs cation vacancies in the support and rebuilds the surface lattice, yielding the single-atom materials with enhanced thermal stability. High-temperature thermal migration excites bulk metals to release migratable metal species, which are captured by the defect-rich supports, thus resulting in single-atom materials. Heteroatom-doped thermal atomization uses high temperatures to break metal-metal bonds in NPs, allowing metal atoms to coordinate with heteroatoms in the support and be anchored on the carbon substrate, hence forming stable single atoms. Based on the analysis presented, the SACs may demonstrate significant potential in the photothermocatalytic oxidation of VOCs.

### Single-atom photothermal catalytic oxidation of VOCs

As an emerging research field, the integration of SACs with photothermal catalysis is in its nascent stage. Single-atom photothermal catalysts have been preliminarily explored for applications in water pollution treatments<sup>[112,113]</sup>, CO<sub>2</sub> reduction<sup>[114]</sup>, catalytic oxidation<sup>[46]</sup>, and biomedical applications<sup>[115]</sup>. Such a technology holds a significant potential for further research in the treatments of VOCs.

#### *Photo-derived thermocatalytic oxidation of VOCs*

Single-atom photothermal catalysts require a support to function, and they serve as enhancers rather than replacements for traditional photothermal catalysts. By loading metal atoms on the supports with superior photothermal conversion properties, catalytic performance of the single-atoms is preserved, and the low catalytic activities of the supports are compensated, thereby harnessing green solar energy effectively. Specifically, single atoms are dispersed on the supports with photothermal conversion properties, such as carbon-based materials (e.g., graphene and CNTs) and metal oxides (TiO<sub>2</sub>, CeO<sub>2</sub>, Fe<sub>2</sub>O<sub>3</sub>, etc.)<sup>[116]</sup>. The IR thermal imaging visualization has shown that the surface temperature of stable, uniformly dispersed graphene-like anchored K SACs reached 73.8 °C under the irradiation of light (1,500 W·m<sup>-2</sup>)<sup>[117]</sup>. Additionally, Pd SACs (Pd<sub>1</sub>/N-graphene) dispersed on Ni-doped graphene achieved a surface temperature of 125 °C under the irradiation of UV light (540 mW·cm<sup>-2</sup>), enabling the efficient CH<sub>2</sub>=CH<sub>2</sub> conversion. The strong local coordination of Ni-Pd prevented Pd aggregation, ensuring good stability of the catalyst<sup>[118]</sup>. The Fe<sub>2</sub>O<sub>3</sub>-supported Pt SACs<sup>[46]</sup> demonstrated photo-driven thermocatalytic activity in converting 200 ppm toluene under the irradiation of light (720 mW·cm<sup>-2</sup>). Under these conditions, toluene conversion and CO<sub>2</sub> yield reached 95% and 87% [Figure 10A], respectively. Research results indicated that the incorporation of single-atom Pt did not improve the photocatalytic performance. Rather, it transformed solar energy into thermal energy, achieving a rapid temperature increase to 210 °C under the light irradiation, which resulted in the oxidation of toluene. In the photo-driven thermocatalysis, achieving catalyst temperatures above 200 °C typically requires intense optical power density, usually exceeding 1 W·cm<sup>-2</sup> (about ten times the standard solar intensity). Researchers developed a dual single-atom strategy to mitigate this requirement. Such a strategy involves adding a second single-atom metal to SACs, creating atomically dispersed multi-metal sites. The aim is to optimize the active site centers, coordination environments, electronic structures, and reactant adsorption/activation capabilities. Mo *et al.* synthesized a stable N-coordinated Ni and Fe dual single-atom [(Ni, Fe)-N-C] on carbon materials. Under the irradiation of light (49.0 mW·cm<sup>-2</sup>), this catalyst reached the surface temperatures above 300 °C without additional energy, effectively driving the thermocatalytic reactions<sup>[119]</sup>. Besides enhancing the photothermal conversion efficiency, minimizing heat loss during these reactions is crucial. Researchers developed Fe-CeO<sub>2</sub> SACs and Ti foil heterostructure catalysts, and found that the high oxidation state of the Fe single-atom reduced the reaction barrier for ethanol decomposition. Additionally, the heterostructure significantly decreased the IR radiation loss, hence optimizing thermal energy utilization in the photo-derived thermocatalysis<sup>[120]</sup>.

#### *Photothermocatalytic oxidation of VOCs*

The photochemical effect is crucial in the photothermocatalytic oxidation. As shown in Figure 10B, the presence or absence of light significantly affected the oxidation of toluene over the Pt<sub>1</sub>/CuO-CeO<sub>2</sub> (Pt<sub>1</sub>/CC) SACs at the same reaction temperature<sup>[121]</sup>. The excellent catalytic activity was associated with the synergistic effect of photo- and thermocatalysis. The loading of single-atom alters the band structure of a catalyst, thus promoting electron-hole separation and aiding the progress of the surface fundamental steps. Studies indicated that the loading of Ru single-atom and Mg-doping both inhibited the recombination of electrons and holes in the Ru<sub>1</sub>/Mg-CeO<sub>2</sub> SACs, making it more likely to participate in the surface reactions and effectively promoting the reaction under the photothermocatalytic conditions<sup>[122,123]</sup>. Under identical external field conditions, the SACs demonstrated superior performance compared to the supported metal NP catalysts. As illustrated in Figure 10C, the conversion of heptane over the Pt<sub>1</sub>/CC SACs could be up to 55%



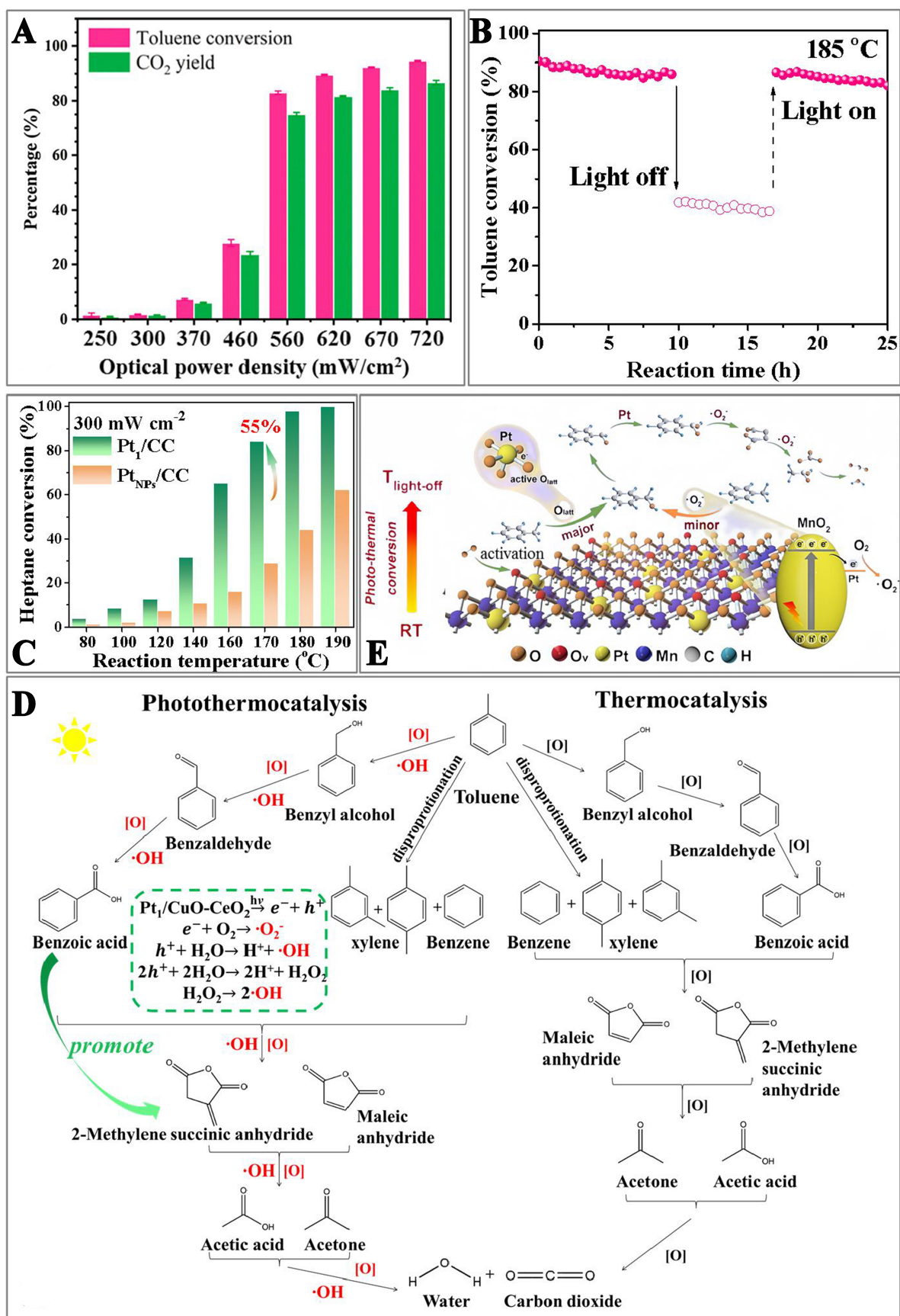


**Figure 10.** (A) Toluene conversion and CO<sub>2</sub> yield over Pt<sub>1</sub>/Fe<sub>2</sub>O<sub>3</sub> under the irradiation of simulated sunlight with different optical power densities<sup>[46]</sup>. Copyright 2021 Elsevier; (B) Long-term stability test for toluene conversion over the Pt SACs with or without irradiation<sup>[121]</sup>. Copyright 2022 American Chemical Society; (C) Heptane conversion over the Pt<sub>1</sub>/CC and Pt<sub>NPs</sub>/CC catalysts as a function of temperature with irradiation<sup>[24]</sup>. Copyright 2023 Elsevier; (D) Mechanism of photothermocatalytic and thermocatalytic toluene oxidation over the 0.39Pt<sub>1</sub>/CC catalyst<sup>[121]</sup>. Copyright 2022 American Chemical Society; and (E) Schematic diagram of the photothermocatalysis mechanism of toluene oxidation on Pt-MnO<sub>2</sub> SACs<sup>[125]</sup>. Copyright 2023 Elsevier. SACs: Single-atom catalysts; Pt<sub>1</sub>/CC: Pt<sub>1</sub>/CuO-CeO<sub>2</sub>; Pt<sub>NPs</sub>/CC: Pt<sub>NPs</sub>/CuO-CeO<sub>2</sub>.

higher than that over the Pt<sub>NPs</sub>/CuO-CeO<sub>2</sub> (Pt<sub>NPs</sub>/CC) catalyst<sup>[24]</sup>. Research revealed that under the light irradiation, the SAC surface generated a more amount of reactive oxygen species (O<sub>2</sub><sup>•</sup> and <sup>•</sup>OH). The oxygen species facilitated the activation of VOC molecules. Additionally, the moderate adsorption of heptane and strong activation of gaseous oxygen of Pt<sub>1</sub>/CC enable rapid and complete oxidation of heptane. In contrast, the limited oxygen activation capability of Pt<sub>NPs</sub>/CC struggled to fully react with the excessively adsorbed VOCs, leading to the accumulation of intermediate products and a decrease in catalytic performance. The Pt<sub>1</sub>/WO<sub>3</sub>-TiO<sub>2</sub> SACs also exhibited significantly higher activity in the photothermocatalytic oxidation of short-chain alkanes (e.g., C<sub>3</sub>H<sub>8</sub> and C<sub>3</sub>H<sub>6</sub>) compared to the corresponding Pt<sub>NPs</sub>/WO<sub>3</sub>-TiO<sub>2</sub> catalyst<sup>[124]</sup>. For C<sub>3</sub>H<sub>6</sub> oxidation, the photothermocatalysis over the Pt<sub>NPs</sub>/WO<sub>3</sub>-TiO<sub>2</sub> catalyst was almost ineffective due to the strong adsorption of C<sub>3</sub>H<sub>6</sub> molecules on Pt NPs (which resulted in catalyst poisoning). In comparison, the oxidation of C<sub>3</sub>H<sub>6</sub> over the Pt<sub>1</sub>/WO<sub>3</sub>-TiO<sub>2</sub> catalyst significantly increased under exposure to light, overcoming C<sub>3</sub>H<sub>6</sub> poisoning, with the appropriated affinity between C<sub>3</sub>H<sub>6</sub> molecules and Pt single-atom being the decisive factor.

In single-atom photothermocatalysis for VOCs oxidation, the focus is not only on adjusting reactant adsorption to promote the reactions but also on controlling the reaction pathways via the consumption of photogenerated carriers. Taking toluene (the typical aromatic compound) as an example, studies showed that over the Pt SACs, the intermediate products of toluene oxidation were the same under both thermal and photothermal conditions. However, as shown in Figure 10D, when light was introduced to the surface of the catalyst, toluene was oxidized by a large number of reactive oxygen species, producing a significant amount of carboxylates. Benzoic acid, an important intermediate before toluene ring opening, was a favored intermediate after the introduction of light (which promoted the conversion of toluene to benzoic acid). Compared to thermocatalysis, light illumination could release the active sites on the catalyst surface, thus increasing the reaction rate<sup>[121]</sup>. This conclusion was further verified in the subsequent studies, where the introduction of single-atom Pt enhanced the activity of surface lattice oxygen on MnO<sub>2</sub>, promoting the formation of benzoic acid and the total mineralization of toluene<sup>[125]</sup>. Additionally, during the photocatalysis process, the Pt single atoms accelerated the formation of O<sub>2</sub><sup>•</sup>, aiding in the ring opening and deep oxidation of toluene [Figure 10E]. The combination of experiments and DFT calculations revealed the synergistic mechanism of photo- and thermocatalysis during the photothermocatalytic process, providing new insights into designing efficient catalysts. The elimination temperatures of VOCs by single-atom photothermal catalysts are compared and recorded in Table 1.

## CONCLUSION AND OUTLOOK

Maximizing the utilization efficiency of metal atoms in catalysts and using solar energy to replace or assist fossil fuels in eliminating VOCs align with the concepts of energy conservation, emission reduction, and green catalysis. In recent years, researchers have extensively studied both single-atom catalytic materials and photothermal catalytic oxidation of VOCs, achieving significant results. However, the field combining single-atom with the photothermal catalytic technology is immature, particularly in the applications involving energy conversion and environmental remediation. The potential of single-atom photothermal catalysts remains largely untapped, and there is a significant gap in understanding their actual contributions

**Table 1. Performance of single-atom photothermal catalysts for VOCs oxidation**

Catalyst	Catalysis mode	Optical power density	VOCs	$c_{\text{VOC}}$ (ppm)	GHSV (mL/g·h)	$T_{90\%}$ (°C)	Ref.
0.25Pt <sub>i</sub> /Fe <sub>2</sub> O <sub>3</sub>	Photo-driven thermocatalysis	720 mW·cm <sup>-2</sup>	Toluene	200	20,000	210	[46]
0.5Pt <sub>i</sub> /Fe <sub>2</sub> O <sub>3</sub>	Photo-driven thermocatalysis	620 mW·cm <sup>-2</sup>	Toluene	200	20,000	190	[46]
0.11Pt <sub>i</sub> /MnO <sub>2</sub>	Photo-driven thermocatalysis	300 mW·cm <sup>-2</sup>	Toluene	300	30,000	-112 ( $T_{95\%}$ )	[125]
0.11Pt <sub>i</sub> /MnO <sub>2</sub>	Photo-driven thermocatalysis	600 mW·cm <sup>-2</sup>	Toluene	300	60,000	-151 ( $T_{99\%}$ )	[125]
0.08Pt <sub>i</sub> /CC	Synergistic photothermocatalysis	300 mW·cm <sup>-2</sup>	Heptane	500	20,000	197	[24]
0.20Pt <sub>i</sub> /CC	Synergistic photothermocatalysis	300 mW·cm <sup>-2</sup>	Heptane	500	20,000	175	[24]
0.42Pt <sub>i</sub> /CC	Synergistic photothermocatalysis	300 mW·cm <sup>-2</sup>	Heptane	500	20,000	186	[24]
0.17Pt <sub>i</sub> /CC	Synergistic photothermocatalysis	200 mW·cm <sup>-2</sup>	Toluene	200	20,000	197	[121]
0.39Pt <sub>i</sub> /CC	Synergistic photothermocatalysis	200 mW·cm <sup>-2</sup>	Toluene	200	20,000	186	[121]
0.83Pt <sub>i</sub> /CC	Synergistic photothermocatalysis	200 mW·cm <sup>-2</sup>	Toluene	200	20,000	174	[121]
0.04Pt <sub>i</sub> /WO <sub>3</sub> -TiO <sub>2</sub>	Synergistic photothermocatalysis	-	Propane	10,000	-	240 [reaction rate 3,792 (μmol/g <sub>Pt</sub> ·s)]	[124]

The  $c_{\text{VOC}}$  represents the concentration of VOCs. VOCs: Volatile organic compounds; GHSV: gas hourly space velocity.

to enhancing photothermal catalytic performance. Therefore, future research in single-atom photothermal catalytic VOCs oxidation could focus on the following areas:

(i) Development of single-atom photothermal catalysts. Currently, understanding the relationship between the structure and performance of these catalysts involves complex experimental steps, such as synthesis, screening, and optimization. Machine learning, a key artificial intelligence technology, can integrate the theoretical computational data to predict the performance of single-atom photothermal catalysts effectively. This approach possesses a significant potential to guide the design of optimal catalyst structures. Insights gained from artificial intelligence predictions can be invaluable for selecting and designing catalysts that improve performance and structural stability.

(ii) Mechanisms of single-atom photothermal effects. There is an urgent need to employ a combination of various *in situ* characterization to investigate the mechanisms of single-atom photothermal catalytic systems. For instance, developing techniques [e.g., *in situ* transmission electron microscopy (TEM), near-ambient X-ray photoelectron spectroscopy (XPS), and *in situ* Raman spectroscopy] is essential for exploring the coordination environments of single atoms and monitoring changes in the active sites. Furthermore, developing spectral techniques such as IR cameras and ultrafast Raman thermometry to measure the local heating and electron transfer processes can deepen the understanding of the fundamental mechanisms.

(iii) Actual condition performance testing. The SACs in both photo-derived thermocatalytic and photothermal catalytic oxidation systems have not been sufficiently evaluated under the actual conditions. In the actual industrial emissions, VOCs are usually diverse and complex, and often accompanied by large amounts of water vapor, chlorinated VOCs, sulfur-containing VOCs, and NO<sub>x</sub>. Therefore, assessing the performance of single-atom photothermal catalysts for the multi-component VOCs removal under realistic conditions is essential.

(iv) Sustainable photothermal catalytic system. Photothermal system faces limitations due to the factors, such as the angle and intensity of natural light and the discontinuity caused by day-night cycles. From both industrial and economic viewpoints, developing the catalysts and reactors capable of efficient catalysis under mild light illumination conditions and maintaining performance in darkness would be of significant practical importance. Such advancements in the above aspects would substantially contribute to global energy conservation and emissions reduction goals.

## DECLARATIONS

### Authors' contributions

Topic proposal: Dai, H.

Manuscript preparation: Feng, Y.

Collective discussion and revision: Chu, P.; Hou, Z.; Wu, L.

Review and editing, methodology, supervision, project administration, funding acquisition: Liu, Y.; Deng, J.; Dai, H.

### Availability of data and materials

Not applicable.

### Financial support and sponsorship

This work was financially supported by the National Natural Science Foundation of China (22425601, U23A20120, 21976009, and 21961160743), National Natural Science Committee of China - Liaoning Provincial People's Government Joint Fund (U1908204), National Key R&D Program of China (2023YFB3810801, 2022YFB3504101, and 2022YFB3506200), R&D Program of Beijing Municipal Education Commission (KZ202210005011), Postdoctoral Science Foundation of China (2022M720315), and Postdoctoral Research Foundation of Beijing (2023ZZ-139).

### Conflicts of interest

All authors declared that there are no conflicts of interest.

### Ethical approval and consent to participate

Not applicable.

### Consent for publication

Not applicable.

### Copyright

© The Author(s) 2025.

## REFERENCES

1. Zhao, C.; Yang, L.; Sun, Y.; et al. Atmospheric emissions of hexachlorobutadiene in fine particulate matter from industrial sources. *Nat. Commun.* **2024**, *15*, 4737. DOI PubMed PMC
2. Brunet, C. E.; Marek, R. F.; Stanier, C. O.; Hornbuckle, K. C. Concentrations of volatile methyl siloxanes in New York City reflect emissions from personal care and industrial use. *Environ. Sci. Technol.* **2024**, *58*, 8835-45. DOI PubMed PMC
3. Pfannerstill, E. Y.; Arata, C.; Zhu, Q.; et al. Comparison between spatially resolved airborne flux measurements and emission inventories of volatile organic compounds in Los Angeles. *Environ. Sci. Technol.* **2023**, *57*, 15533-45. DOI
4. He, Z.; Liu, P.; Zhao, X.; He, X.; Liu, J.; Mu, Y. Responses of surface O<sub>3</sub> and PM<sub>2.5</sub> trends to changes of anthropogenic emissions in summer over Beijing during 2014-2019: a study based on multiple linear regression and WRF-Chem. *Sci. Total. Environ.* **2022**, *807*,



150792. DOI PubMed
5. Liu, S.; Li, X.; Wei, J.; et al. Short-term exposure to fine particulate matter and ozone: source impacts and attributable mortalities. *Environ. Sci. Technol.* **2024**, *58*, 11256-67. DOI PubMed PMC
  6. Chu, P.; Zhang, L.; Wang, Z.; et al. Regulation lattice oxygen mobility via dual single atoms for simultaneously enhancing VOC oxidation and NO<sub>x</sub> reduction. *Environ. Sci. Technol.* **2024**, *58*, 17475-84. DOI PubMed
  7. Guo, M.; Ma, P.; Wang, J.; et al. Synergy in Au-CuO Janus structure for catalytic isopropanol oxidative dehydrogenation to acetone. *Angew. Chem. Int. Ed. Engl.* **2022**, *61*, e202203827. DOI PubMed
  8. Zhang, H.; Dai, L.; Feng, Y.; et al. A Resource utilization method for volatile organic compounds emission from the semiconductor industry: selective catalytic oxidation of isopropanol to acetone over Au/ $\alpha$ -Fe<sub>2</sub>O<sub>3</sub> nanosheets. *Appl. Catal. B. Environ.* **2020**, *275*, 119011. DOI
  9. He, C.; Cheng, J.; Zhang, X.; Douthwaite, M.; Pattison, S.; Hao, Z. Recent advances in the catalytic oxidation of volatile organic compounds: a review based on pollutant sorts and sources. *Chem. Rev.* **2019**, *119*, 4471-568. DOI
  10. Gunathilake, C.; Soliman, I.; Panthi, D.; et al. A comprehensive review on hydrogen production, storage, and applications. *Chem. Soc. Rev.* **2024**, *53*, 10900-69. DOI
  11. Miao, R.; He, Z.; Wu, B.; et al. Activated carbon-boosted BiOI in CO<sub>2</sub> adsorption and electron transfer for photothermally catalyzed CO<sub>2</sub> oxidative dehydrogenation of propane. *Chem. Eng. J.* **2024**, *481*, 148293. DOI
  12. Guo, M.; Ma, P.; Wei, L.; et al. Highly selective activation of C-H bond and inhibition of C-C bond cleavage by tuning strong oxidative Pd sites. *J. Am. Chem. Soc.* **2023**, *145*, 11110-20. DOI
  13. Rao, Z.; Wang, K.; Cao, Y.; et al. Light-reinforced key intermediate for anticoking to boost highly durable methane dry reforming over single atom Ni active sites on CeO<sub>2</sub>. *J. Am. Chem. Soc.* **2023**, *145*, 24625-35. DOI
  14. Zhang, Y.; Wang, Y.; Xie, R.; et al. Photocatalytic oxidation for volatile organic compounds elimination: from fundamental research to practical applications. *Environ. Sci. Technol.* **2022**, *56*, 16582-601. DOI
  15. Sun, X.; Feng, Z.; Wang, S.; et al. Insight into the role of TiO<sub>2</sub> facets in photocatalytic selective oxidation of *p*-xylene. *ACS. Catal.* **2024**, *14*, 5356-65. DOI
  16. Yuan, S.; Bao, X.; Chen, M.; et al. Unravelling the pathway determining the CO<sub>2</sub> selectivity in photocatalytic toluene oxidation on TiO<sub>2</sub> with different particle size. *Chem. Eng. J.* **2023**, *470*, 144138. DOI
  17. Liu, B.; Zhang, B.; Liu, B.; et al. Surface hydroxyl and oxygen vacancies engineering in ZnSnAl LDH: synergistic promotion of photocatalytic oxidation of aromatic VOCs. *Environ. Sci. Technol.* **2024**, *58*, 4404-14. DOI
  18. Zhang, H.; Gao, Y.; Meng, S.; et al. Metal sulfide S-scheme homojunction for photocatalytic selective phenylcarbinol oxidation. *Adv. Sci.* **2024**, *11*, 2400099. DOI PubMed PMC
  19. Mehmood, S.; Sk, S.; Abraham, B. M.; Ahmadipour, M.; Pal, U.; Dutta, J. Recent advances in single-atom catalyst for solar energy conversion: a comprehensive review and future outlook. *Adv. Funct. Mater.* **2024**, 2418602. DOI
  20. Dong, Y.; Song, R.; Zhang, Z.; et al. Advances in photothermal CO<sub>2</sub> hydrogenation catalysis for C1 molecules. *Cell. Rep. Phys. Sci.* **2024**, *5*, 102227. DOI
  21. Zhang, Z.; Han, X.; Zhang, J.; et al. Revolutionizing photothermal CO<sub>2</sub> hydrogenation with ceria-based catalysts. *Nano. Res.* **2025**, *18*, 94906998. DOI
  22. Sun, J.; Lian, G.; Chen, Z.; Zou, Z.; Wang, L. Merger of single-atom catalysis and photothermal catalysis for future chemical production. *ACS. Nano.* **2024**, *18*, 34572-95. DOI
  23. Wang, X.; Li, Z.; Gao, R.; et al. Photothermal catalytic removal of 1,2-DCE with high HCl selectivity over the Brønsted acid-enriched sulfur-doped MOFs. *Environ. Sci. Technol.* **2024**, *58*, 17190-200. DOI
  24. Feng, Y.; Wang, Z.; Hua, M.; et al. Differences between atomically-dispersed and particulate Pt supported catalysts on synergistic photothermocatalytic oxidation of VOCs from cooking oil fumes. *Appl. Catal. B. Environ.* **2023**, *339*, 123116. DOI
  25. Cheng, Q.; Yang, Z.; Li, Y.; Wang, J.; Wang, J.; Zhang, G. Amorphous/crystalline Cu<sub>1.5</sub>Mn<sub>1.5</sub>O<sub>4</sub> with rich oxygen vacancies for efficiently photothermocatalytic mineralization of toluene. *Chem. Eng. J.* **2023**, *471*, 144295. DOI
  26. Wu, J.; Xiong, L.; Zhao, B.; Liu, M.; Huang, L. Densely populated single atom catalysts. *Small. Methods.* **2020**, *4*, 1900540. DOI
  27. Maschmeyer, T.; Rey, F.; Sankar, G.; Thomas, J. M. Heterogeneous catalysts obtained by grafting metallocene complexes onto mesoporous silica. *Nature* **1995**, *378*, 159-62. DOI
  28. Asakura, K.; Nagahiro, H.; Ichikuni, N.; Iwasawa, Y. Structure and catalytic combustion activity of atomically dispersed Pt species at MgO surface. *Appl. Catal. A. Gen.* **1999**, *188*, 313-24. DOI
  29. Hackett, S. F.; Brydson, R. M.; Gass, M. H.; et al. High-activity, single-site mesoporous Pd/Al<sub>2</sub>O<sub>3</sub> catalysts for selective aerobic oxidation of allylic alcohols. *Angew. Chem. Int. Ed. Engl.* **2007**, *46*, 8593-6. DOI
  30. Kwak, J. H.; Hu, J.; Mei, D.; et al. Coordinatively unsaturated Al<sup>3+</sup> centers as binding sites for active catalyst phases of platinum on  $\gamma$ -Al<sub>2</sub>O<sub>3</sub>. *Science* **2009**, *325*, 1670-3. DOI
  31. Qiao, B.; Wang, A.; Yang, X.; et al. Single-atom catalysis of CO oxidation using Pt/FeO<sub>x</sub>. *Nat. Chem.* **2011**, *3*, 634-41. DOI
  32. Liang, X.; Fu, N.; Yao, S.; Li, Z.; Li, Y. The progress and outlook of metal single-atom-site catalysis. *J. Am. Chem. Soc.* **2022**, *144*, 18155-74. DOI
  33. Chen, Y.; Lin, J.; Jia, B.; Wang, X.; Jiang, S.; Ma, T. Isolating single and few atoms for enhanced catalysis. *Adv. Mater.* **2022**, *34*, e2201796. DOI
  34. Lowe, B.; Hellerstedt, J.; Matěj, A.; et al. Selective activation of aromatic C-H bonds catalyzed by single gold atoms at room

- temperature. *J. Am. Chem. Soc.* **2022**, *144*, 21389-97. DOI
35. Zhou, J.; Pan, J.; Jin, Y.; et al. Single-cation catalyst: Ni cation in monolayered CuO for CO oxidation. *J. Am. Chem. Soc.* **2022**, *144*, 8430-3. DOI
36. Cui, T.; Li, L.; Ye, C.; et al. Heterogeneous single atom environmental catalysis: fundamentals, applications, and opportunities. *Adv. Funct. Mater.* **2022**, *32*, 2108381. DOI
37. Gong, S.; Ni, B.; He, X.; et al. Electronic modulation of a single-atom-based tandem catalyst boosts CO<sub>2</sub> photoreduction to ethanol. *Energy. Environ. Sci.* **2023**, *16*, 5956-69. DOI
38. Xu, H.; Cheng, D.; Cao, D.; Zeng, X. C. Revisiting the universal principle for the rational design of single-atom electrocatalysts. *Nat. Catal.* **2024**, *7*, 207-18. DOI
39. Li, X.; Pereira-Hernández, X. I.; Chen, Y.; et al. Functional CeO<sub>x</sub> nanoglues for robust atomically dispersed catalysts. *Nature* **2022**, *611*, 284-8. DOI
40. Qian, M.; Wu, X.; Lu, M.; et al. Modulation of charge trapping by island-like single-atom cobalt catalyst for enhanced photo-fenton-like reaction. *Adv. Funct. Mater.* **2023**, *33*, 2208688. DOI
41. Shi, Y.; Zhou, Y.; Lou, Y.; Chen, Z.; Xiong, H.; Zhu, Y. Homogeneity of supported single-atom active sites boosting the selective catalytic transformations. *Adv. Sci.* **2022**, *9*, 2201520. DOI PubMed PMC
42. Guo, Y.; Huang, Y.; Zeng, B.; et al. Photo-thermo semi-hydrogenation of acetylene on Pd<sub>1</sub>/TiO<sub>2</sub> single-atom catalyst. *Nat. Commun.* **2022**, *13*, 2648. DOI PubMed PMC
43. Xie, B.; Hu, D.; Kumar, P.; Ordonsky, V. V.; Khodakov, A. Y.; Amal, R. Heterogeneous catalysis via light-heat dual activation: a path to the breakthrough in C1 chemistry. *Joule* **2024**, *8*, 312-33. DOI
44. Wei, L.; Yu, C.; Yang, K.; Fan, Q.; Ji, H. Recent advances in VOCs and CO removal via photothermal synergistic catalysis. *Chin. J. Catal.* **2021**, *42*, 1078-95. DOI
45. Qin, X.; Xu, M.; Guan, J.; et al. Direct conversion of CO and H<sub>2</sub>O to hydrocarbons at atmospheric pressure using a TiO<sub>2-x</sub>/Ni photothermal catalyst. *Nat. Energy* **2024**, *9*, 154-62. DOI
46. Wang, Z.; Xie, S.; Feng, Y.; et al. Simulated solar light driven photothermal catalytic purification of toluene over iron oxide supported single atom Pt catalyst. *Appl. Catal. B. Environ.* **2021**, *298*, 120612. DOI
47. Vikrant, K.; Weon, S.; Kim, K.; Sillanpää, M. Platinized titanium dioxide (Pt/TiO<sub>2</sub>) as a multi-functional catalyst for thermocatalysis, photocatalysis, and photothermal catalysis for removing air pollutants. *Appl. Mater. Today* **2021**, *23*, 100993. DOI
48. Yu, X.; Fan, S.; Zhu, B.; El-Hout, S. I.; Zhang, J.; Chen, C. Recent progress on photothermal nanomaterials: design, mechanism, and applications. *Green. Energy. Environ.* **2024**. DOI
49. Wang, M.; Jia, J.; Meng, Z.; et al. Plasmonic Pd-Sb nanosheets for photothermal CH<sub>4</sub> conversion to HCHO and therapy. *Sci. Adv.* **2024**, *10*, eado9664. DOI PubMed PMC
50. Zhou, L.; Huang, Q.; Xia, Y. Plasmon-induced hot electrons in nanostructured materials: generation, collection, and application to photochemistry. *Chem. Rev.* **2024**, *124*, 8597-619. DOI PubMed PMC
51. Lee, A.; Wu, S.; Yim, J. E.; Zhao, B.; Sheldon, M. T. Hot electrons in a steady state: interband vs intraband excitation of plasmonic gold. *ACS. Nano* **2024**, *18*, 19077-85. DOI PubMed PMC
52. Dong, S.; Zhao, Y.; Yang, J.; et al. Visible-light responsive PDI/rGO composite film for the photothermal catalytic degradation of antibiotic wastewater and interfacial water evaporation. *Appl. Catal. B. Environ.* **2021**, *291*, 120127. DOI
53. Xiang, Z.; Shi, Y.; Zhu, X.; Cai, L.; Lu, W. Flexible and waterproof 2D/1D/0D construction of MXene-based nanocomposites for electromagnetic wave absorption, EMI shielding, and photothermal conversion. *Nanomicro. Lett.* **2021**, *13*, 150. DOI PubMed PMC
54. Zhou, J.; Liu, H.; Wang, H. Photothermal catalysis for CO<sub>2</sub> conversion. *Chin. Chem. Lett.* **2023**, *34*, 107420. DOI
55. Anderson, C. L.; Zhang, T.; Qi, M.; et al. Exceptional electron-rich heteroaromatic pentacycle for ultralow band gap conjugated polymers and photothermal therapy. *J. Am. Chem. Soc.* **2023**, *145*, 5474-85. DOI
56. Shi, Y.; Wang, Y.; Meng, N.; Liao, Y. Photothermal conversion porous organic polymers: design, synthesis, and applications. *Small. Methods* **2024**, *8*, e2301554. DOI
57. Liu, Z.; Niu, L.; Zong, X.; et al. Ambient photothermal catalytic CO oxidation over a carbon-supported palladium catalyst. *Appl. Catal. B. Environ.* **2022**, *313*, 121439. DOI
58. Elimian E, Zhang M, Sun Y, He J, Jia H. Harnessing solar energy towards synergistic photothermal catalytic oxidation of volatile organic compounds. *Solar. RRL* **2023**, *7*, 2300238. DOI
59. Chen, X.; Cai, S.; Yu, E.; Li, J.; Chen, J.; Jia, H. Photothermocatalytic performance of ACo<sub>2</sub>O<sub>4</sub> type spinel with light-enhanced mobilizable active oxygen species for toluene oxidation. *Appl. Surf. Sci.* **2019**, *484*, 479-88. DOI
60. Li, J.; Yu, E.; Cai, S.; et al. Noble metal free, CeO<sub>2</sub>/LaMnO<sub>3</sub> hybrid achieving efficient photo-thermal catalytic decomposition of volatile organic compounds under IR light. *Appl. Catal. B. Environ.* **2019**, *240*, 141-52. DOI
61. Li, Y.; Liu, B.; Yuan, D.; et al. High-purity carbon monoxide production via photothermal formic acid decomposition over fluorite ZrO<sub>2</sub>. *Nat. Catal.* **2024**, *7*, 1350-8. DOI
62. Shi, H.; Tian, C.; Liu, X.; et al. Ni-phyllsilicate nanotubes coated by CeO<sub>2</sub> for ultra-efficiency of 36.9% and near-limit CO<sub>2</sub> conversion in solar-driven conversion of CO<sub>2</sub>-to-fuel. *Chem. Eng. J.* **2023**, *454*, 140063. DOI
63. Chai, H.; Xu, J.; Zhang, Z.; et al. Tuning surface defects of WO<sub>3-x</sub> for enhanced photothermal catalytic propane combustion. *Appl. Surf. Sci.* **2024**, *657*, 159709. DOI

64. Ren, S.; Han, J.; Yang, Z.; et al. Near-unity photothermal CO<sub>2</sub> hydrogenation to methanol based on a molecule/nanocarbon hybrid catalyst. *Angew. Chem. Int. Ed. Engl.* **2025**, *64*, e202416376. DOI
65. Zhang, Z.; Mao, C.; Meira, D. M.; et al. New black indium oxide-tandem photothermal CO<sub>2</sub>-H<sub>2</sub> methanol selective catalyst. *Nat. Commun.* **2022**, *13*, 1512. DOI PubMed PMC
66. Cheng, Q.; Wang, K.; Yang, Z.; Li, Y.; Zhang, G. Surface oxygen vacancies induced by Cu-doping in hexagonal ZnMn<sub>2</sub>O<sub>4</sub> nanoplates for high efficiency photothermocatalytic oxidation of toluene. *Sep. Purif. Technol.* **2025**, *354*, 128743. DOI
67. Fang, H.; Kang, Y.; Yuan, S.; Zhang, M.; Rui, Z. One step synthesis and interfacial properties of black Ag/TiO<sub>2-x</sub> for enhancing sunlight absorption with application to photothermocatalytic VOCs degradation. *Appl. Surf. Sci.* **2024**, *655*, 159519. DOI
68. Mo, S.; Zhao, X.; Huang, L.; et al. Uncovering the role of unsaturated coordination defects in manganese oxides for concentrated solar-heating photothermal OVOCs oxidation: experimental and DFT explorations. *Appl. Catal. B. Environ.* **2024**, *342*, 123435. DOI
69. Elimian, E. A.; Zhang, M.; Chen, J.; Jia, H.; Sun, Y.; He, J. Construction of Pt-mTiO<sub>2</sub>/USY multifunctional catalyst enriched with oxygen vacancies for the enhanced light-driven photothermocatalytic degradation of toluene. *Appl. Catal. B. Environ.* **2022**, *307*, 121203. DOI
70. Zhang, J.; Chen, H.; Duan, X.; Sun, H.; Wang, S. Photothermal catalysis: from fundamentals to practical applications. *Mater. Today.* **2023**, *68*, 234-53. DOI
71. Liu, S.; Wang, X.; Chen, Y.; et al. Efficient thermal management with selective metamaterial absorber for boosting photothermal CO<sub>2</sub> hydrogenation under sunlight. *Adv. Mater.* **2024**, *36*, e2311957. DOI
72. Yang, Z.; Wu, Z. Y.; Lin, Z.; et al. Optically selective catalyst design with minimized thermal emission for facilitating photothermal catalysis. *Nat. Commun.* **2024**, *15*, 7599. DOI PubMed PMC
73. Du, K.; Guo, J.; Song, C.; et al. Persistent photothermal CO<sub>2</sub> methanation without external energy input. *Energy. Environ. Sci.* **2025**, *18*, 1255-61. DOI
74. Liu, B.; Wu, H.; Parkin, I. P. Gaseous photocatalytic oxidation of formic acid over TiO<sub>2</sub>: a comparison between the charge carrier transfer and light-assisted Mars-van Krevelen pathways. *J. Phys. Chem. C.* **2019**, *123*, 22261-72. DOI
75. Feng, Y.; Ma, P.; Wang, Z.; et al. Synergistic effect of reactive oxygen species in photothermocatalytic removal of VOCs from cooking oil fumes over Pt/CeO<sub>2</sub>/TiO<sub>2</sub>. *Environ. Sci. Technol.* **2022**, *56*, 17341-51. DOI
76. Jiang, Y.; Li, S.; Wang, S.; et al. Enabling specific photocatalytic methane oxidation by controlling free radical type. *J. Am. Chem. Soc.* **2023**, *145*, 2698-707. DOI
77. Song, C.; Wang, Z.; Yin, Z.; Xiao, D.; Ma, D. Principles and applications of photothermal catalysis. *Chem. Catal.* **2022**, *2*, 52-83. DOI
78. Zhang, J.; Li, Y.; Sun, J.; et al. Regulation of energetic hot carriers on Pt/TiO<sub>2</sub> with thermal energy for photothermal catalysis. *Appl. Catal. B. Environ.* **2022**, *309*, 121263. DOI
79. Lu, J.; Chen, Z.; Shen, Y.; et al. Boosting photothermal-assisted photocatalytic H<sub>2</sub> production over black g-C<sub>3</sub>N<sub>4</sub> nanosheet photocatalyst via incorporation with carbon dots. *J. Colloid. Interface. Sci.* **2024**, *670*, 428-38. DOI
80. Imai, K.; Fukushima, T.; Kobayashi, H.; Higashimoto, S. Visible-light responsive TiO<sub>2</sub> for the complete photocatalytic decomposition of volatile organic compounds (VOCs) and its efficient acceleration by thermal energy. *Appl. Catal. B. Environ. Energy.* **2024**, *346*, 123745. DOI
81. He, T.; Rong, S.; Ding, D.; Zhou, Y.; Zhang, N.; He, W. Facet-controlled synthesis of Mn<sub>3</sub>O<sub>4</sub> nanorods for photothermal synergistic catalytic oxidation of carcinogenic airborne formaldehyde. *ACS. Catal.* **2023**, *13*, 8049-62. DOI
82. Feng, X.; Liu, D.; Yan, B.; et al. Highly active PdO/Mn<sub>3</sub>O<sub>4</sub>/CeO<sub>2</sub> nanocomposites supported on one dimensional halloysite nanotubes for photoassisted thermal catalytic methane combustion. *Angew. Chem. Int. Ed. Engl.* **2021**, *60*, 18552-6. DOI
83. Tang, Y.; Wu, S.; Wang, Y.; et al. Photo-assisted catalytic CO<sub>2</sub> hydrogenation to CO with nearly 100% selectivity over Rh/TiO<sub>2</sub> catalysts. *Energy. Fuels.* **2023**, *37*, 539-46. DOI
84. Song, X.; Fan, S.; Cai, Z.; et al. NH<sub>3</sub> synthesis via visible-light-assisted thermocatalytic NO reduction by CO in the presence of H<sub>2</sub>O over Cu/CeO<sub>2</sub>. *Chin. J. Catal.* **2023**, *49*, 168-79. DOI
85. Ning, S.; Ou, H.; Li, Y.; et al. Co<sup>0</sup>-Co<sup>δ+</sup> interface double-site-mediated C-C coupling for the photothermal conversion of CO<sub>2</sub> into light olefins. *Angew. Chem. Int. Ed. Engl.* **2023**, *62*, e202302253. DOI
86. Wang, S.; Yuan, F.; Liang, J.; et al. Enhanced photo-assisted thermal catalytic oxidation of formaldehyde via abundant surface adsorbed oxygen in Co<sub>3</sub>O<sub>4</sub> with the assistance of natural zeolite. *Micropor. Mesopor. Mat.* **2025**, *382*, 113401. DOI
87. Yang, Y.; Zhao, S.; Bi, F.; et al. Highly efficient photothermal catalysis of toluene over Co<sub>3</sub>O<sub>4</sub>/TiO<sub>2</sub> p-n heterojunction: the crucial roles of interface defects and band structure. *Appl. Catal. B. Environ.* **2022**, *315*, 121550. DOI
88. Sun, C.; Zhao, K.; Boies, A.; Xiao, S.; Yi, Z. Boosting total oxidation of methane over NiO nanocrystalline decorated ZnO-CoNi solid solution via photothermal synergism. *Appl. Catal. B. Environ.* **2023**, *339*, 123124. DOI
89. Jiang, S.; Li, C.; Muhammad, Y.; et al. Solvent-induced fabrication of Cu/MnO<sub>x</sub> nanosheets with abundant oxygen vacancies for efficient and long-lasting photothermal catalytic degradation of humid toluene vapor. *Appl. Catal. B. Environ.* **2023**, *328*, 122509. DOI
90. Wang, H.; Zhao, Q.; Li, D.; et al. Boosting photothermocatalytic oxidation of toluene over Pt/N-TiO<sub>2</sub>: the gear effect of light and heat. *Environ. Sci. Technol.* **2024**, *58*, 7662-71. DOI
91. Hao, Y.; Zhang, X.; Zhang, H.; et al. Contributions of surface oxygen species and photoinduced holes on photothermocatalytic toluene oxidation over CeO<sub>2</sub>-MgO. *ACS. Appl. Nano. Mater.* **2023**, *6*, 9385-96. DOI

92. Li, Y.; Zhang, Q.; Chong, Y.; et al. Efficient photothermal catalytic oxidation enabled by three-dimensional nanochannel substrates. *Environ. Sci. Technol.* **2024**, *58*, 5153-61. DOI
93. Zhang, N.; He, W.; Cheng, Z.; et al. Construction of  $\alpha$ -MnO<sub>2</sub>/g-C<sub>3</sub>N<sub>4</sub> Z-scheme heterojunction for photothermal synergistic catalytic decomposition of formaldehyde. *Chem. Eng. J.* **2023**, *466*, 143160. DOI
94. Kang, L.; Liu, X. Y.; Wang, A.; et al. Photo-thermo catalytic oxidation over a TiO<sub>2</sub>-WO<sub>3</sub>-supported platinum catalyst. *Angew. Chem. Int. Ed. Engl.* **2020**, *59*, 12909-16. DOI
95. Ren, Y.; Si, Y.; Du, M.; et al. Photothermal synergistic effect induces bimetallic cooperation to modulate product selectivity of CO<sub>2</sub> reduction on different CeO<sub>2</sub> crystal facets. *Angew. Chem. Int. Ed. Engl.* **2024**, *63*, e202410474. DOI
96. Kong, J.; Song, S.; Zhao, W.; et al. Unraveling a trade-off between positive effect and poisoning mechanism of soot over low-dose PtCu/CeO<sub>2</sub> for simultaneously photothermocatalytic removal of VOCs and soot. *Appl. Catal. B. Environ.* **2023**, *339*, 123118. DOI
97. Zhang, J.; Zhao, C.; Zou, M.; et al. An effective strategy to improve the photothermocatalytic activity of Co<sub>3</sub>O<sub>4</sub> for VOCs degradation: specifically enhancing the surface lattice oxygen activity. *Sep. Purif. Technol.* **2023**, *327*, 124905. DOI
98. Su, D. W.; Ran, J.; Zhuang, Z. W.; et al. Atomically dispersed Ni in cadmium-zinc sulfide quantum dots for high-performance visible-light photocatalytic hydrogen production. *Sci. Adv.* **2020**, *6*, eaaz8447. DOI PubMed PMC
99. Liu, Y.; Sun, Y.; Zhao, E.; et al. Atomically dispersed silver-cobalt dual-metal sites synergistically promoting photocatalytic hydrogen evolution. *Adv. Funct. Mater.* **2023**, *33*, 2301840. DOI
100. Niu, X.; Zhu, Q.; Jiang, S.; Zhang, Q. Photoexcited electron dynamics of nitrogen fixation catalyzed by ruthenium single-atom catalysts. *J. Phys. Chem. Lett.* **2020**, *11*, 9579-86. DOI
101. Xue, Z.; Yang, J.; Ma, L.; et al. Efficient benzylic C-H bond activation over single-atom yttrium supported on TiO<sub>2</sub> via facilitated molecular oxygen and surface lattice oxygen activation. *ACS. Catal.* **2024**, *14*, 249-61. DOI
102. Giulimondi, V.; Mitchell, S.; Pérez-Ramírez, J. Challenges and opportunities in engineering the electronic structure of single-atom catalysts. *ACS. Catal.* **2023**, *13*, 2981-97. DOI PubMed PMC
103. Li, X.; Rong, H.; Zhang, J.; Wang, D.; Li, Y. Modulating the local coordination environment of single-atom catalysts for enhanced catalytic performance. *Nano. Res.* **2020**, *13*, 1842-55. DOI
104. Feng, Y.; Wang, C.; Wang, C.; et al. Catalytic stability enhancement for pollutant removal via balancing lattice oxygen mobility and VOCs adsorption. *J. Hazard. Mater.* **2022**, *424*, 127337. DOI
105. Wu, P.; Jin, X.; Qiu, Y.; Ye, D. Recent progress of thermocatalytic and photo/thermocatalytic oxidation for VOCs purification over manganese-based oxide catalysts. *Environ. Sci. Technol.* **2021**, *55*, 4268-86. DOI PubMed
106. Han, W.; Ling, W.; Gao, P.; Dong, F.; Tang, Z. Engineering Pt single atom catalyst with abundant lattice oxygen by dual nanospace confinement strategy for the efficient catalytic elimination of VOCs. *Appl. Catal. B. Environ.* **2024**, *345*, 123687. DOI
107. Wang, B.; Yang, Q.; Li, B.; et al. Heterostructure-strengthened metal-support interaction of single-atom Pd catalysts enabling efficient oxygen activation for CO and VOC oxidation. *Appl. Catal. B. Environ.* **2023**, *332*, 122753. DOI
108. Fang, Y.; Zhang, Q.; Zhang, H.; et al. Dual activation of molecular oxygen and surface lattice oxygen in single atom Cu<sub>1</sub>/TiO<sub>2</sub> catalyst for CO oxidation. *Angew. Chem. Int. Ed. Engl.* **2022**, *61*, e202212273. DOI
109. Liu, S.; Niu, S.; Liu, J.; Wang, D.; Wang, Y.; Han, K. Mechanism of formaldehyde oxidation catalyzed by doped graphene single atom catalysts: density functional theory study. *Mol. Catal.* **2022**, *528*, 112516. DOI
110. Lv, H.; Guo, W.; Chen, M.; Zhou, H.; Wu, Y. Rational construction of thermally stable single atom catalysts: from atomic structure to practical applications. *Chin. J. Catal.* **2022**, *43*, 71-91. DOI
111. Hou, Z.; Lu, Y.; Liu, Y.; et al. A general dual-metal nanocrystal dissociation strategy to generate robust high-temperature-stable alumina-supported single-atom catalysts. *J. Am. Chem. Soc.* **2023**, *145*, 15869-78. DOI
112. Xia, D.; Liu, H.; Xu, B.; et al. Single Ag atom engineered 3D-MnO<sub>2</sub> porous hollow microspheres for rapid photothermocatalytic inactivation of *E. coli* under solar light. *Appl. Catal. B. Environ.* **2019**, *245*, 177-89. DOI
113. Xu, W.; Sun, B.; Wu, F.; et al. Manganese single-atom catalysts for catalytic-photothermal synergistic anti-infected therapy. *Chem. Eng. J.* **2022**, *438*, 135636. DOI
114. Cai, S.; Zhang, M.; Li, J.; Chen, J.; Jia, H. Anchoring single-atom Ru on CdS with enhanced CO<sub>2</sub> capture and charge accumulation for high selectivity of photothermocatalytic CO<sub>2</sub> reduction to solar fuels. *Solar. RRL.* **2021**, *5*, 2000313. DOI
115. Feng, Y.; Qin, J.; Zhou, Y.; Yue, Q.; Wei, J. Spherical mesoporous Fe-N-C single-atom nanozyme for photothermal and catalytic synergistic antibacterial therapy. *J. Colloid. Interface. Sci.* **2022**, *606*, 826-36. DOI
116. Wang, Y.; Liu, H.; Shi, Q.; et al. Single-atom titanium on mesoporous nitrogen, oxygen-doped carbon for efficient photo-thermal catalytic CO<sub>2</sub> cycloaddition by a radical mechanism. *Angew. Chem. Int. Ed. Engl.* **2024**, *63*, e202404911. DOI
117. Huang, J.; Liu, T.; Wang, K.; et al. Room-temperature and carbon-negative production of biodiesel via synergy of geminal-atom and photothermal catalysis. *Environ. Chem. Lett.* **2024**, *22*, 1607-13. DOI
118. Zhou, S.; Shang, L.; Zhao, Y.; et al. Pd single-atom catalysts on nitrogen-doped graphene for the highly selective photothermal hydrogenation of acetylene to ethylene. *Adv. Mater.* **2019**, *31*, e1900509. DOI
119. Mo, S.; Zhao, X.; Li, S.; et al. Non-interacting Ni and Fe dual-atom pair sites in N-doped carbon catalysts for efficient concentrating solar-driven photothermal CO<sub>2</sub> reduction. *Angew. Chem. Int. Ed. Engl.* **2023**, *62*, e202313868. DOI
120. Yuan, D.; Han, G.; Wang, Z.; et al. Hybrid structure of iron single atoms and metallic titanium for photothermal ethanol steam reforming. *Sci. China. Chem.* **2024**, *67*, 848-54. DOI
121. Feng, Y.; Dai, L.; Wang, Z.; et al. Photothermal synergistic effect of Pt/CuO-CeO<sub>2</sub> single-atom catalysts significantly improving



- toluene removal. *Environ. Sci. Technol.* **2022**, *56*, 8722-32. DOI
122. Zhang, Z.; Li, T.; Sun, X.; et al. Efficient photo-thermal catalytic CO<sub>2</sub> methanation and dynamic structural evolution over Ru/Mg-CeO<sub>2</sub> single-atom catalyst. *J. Catal.* **2024**, *430*, 115303. DOI
123. Zhang, Z.; Huang, Z.; Yu, X.; et al. Photo-thermal coupled single-atom catalysis boosting dry reforming of methane beyond thermodynamic limits over high equivalent flow. *Nano. Energy.* **2024**, *123*, 109401. DOI
124. Zhu, R.; Kang, L.; Li, L.; et al. Photo-thermo catalytic oxidation of C<sub>3</sub>H<sub>8</sub> and C<sub>3</sub>H<sub>6</sub> over the WO<sub>3</sub>-TiO<sub>2</sub> supported Pt single-atom catalyst. *Acta. Phys. Chim. Sin.* **2024**, *40*, 2303003. DOI
125. Wang, Y.; Dai, J.; Wang, M.; Qi, F.; Jin, X.; Zhang, L. Enhanced toluene oxidation by photothermal synergetic catalysis on manganese oxide embedded with Pt single-atoms. *J. Colloid. Interface. Sci.* **2023**, *636*, 577-87. DOI



Jiguang Deng

Jiguang Deng [College of Materials Science and Engineering, Beijing University of Technology (BJUT)] received his Ph.D. degree from BJUT (China) in 2010. Since then, he has been working at BJUT and is currently a professor. His research interests focus on low-carbon environmental chemistry, environmental catalysis, and photothermal catalysis technologies for the elimination or utilization of typical gaseous pollutants (VOCs, NO<sub>x</sub>, CH<sub>4</sub>, CO<sub>2</sub>, and NH<sub>3</sub>). He has an H-index of 70 and has received over 14,000 citations, according to Scopus.



Hongxing Dai

Hongxing Dai [College of Materials Science and Engineering, Beijing University of Technology (BJUT)] received his Ph.D. degree from Hong Kong Baptist University in 2001. After conducting postdoctoral research at Hong Kong Baptist University, the University of California, Berkeley, and Lawrence Berkeley National Laboratory from 2001 to 2003, he joined Beijing University of Technology as a full professor in 2003. His research interests focus on light alkane oxidation, environmental catalysis, air pollution control, and photocatalysis. He has an H-index of 79 and has received over 19,000 citations, according to Scopus.